DuneFront

Deliverable D5.1

August 2025

DuneFront

Habitat & vegetation evolution in Demonstrators

DuneFront – D5.1

Deliverable information

Title	Habitat & vegetation evolution in Demonstrators
Deliverable number	D5.1
WP number	5
Author(s)	Orane Mordacq (UBx & UGent), Maxime Dahirel (UGent)
Lead beneficiary	UBx
Contributors	
Type	Report
Dissemination level	Public
How to cite	
Copyright license*	© Authors and DuneFront consortium, 2024-2027. *This work is openly licensed via* CC-BY

Versioning and contribution history

Version	Date	Authors (Institution)	Notes
Version 0.1	2025-08-12	UBx, UGent	Draft created by Beneficiary A (UBx)
Version 1.0	2025-09-01	UBx, UGent	Final version approved by all Beneficiaries

Funded by the European Union. Views and opinions expressed are however those of the author(s) only and do not necessarily reflect those of the European Union. Neither the European Union nor the granting authority can be held responsible for them.

Funded by the European Union

DuneFront

Cover page

The goal of the DuneFront project is to develop research on Dune-Dike hybrid (DD-hybrid) Nature-based Solutions (NbS), to improve coastal protection in a context of climate change and rising sea levels. Coastal dunes are important natural habitats that support a wide variety of plant and animal life. The overall objective of the **WP5** is to evaluate **biodiversity** -including habitats and species - across 13 hybrid dune-dike demonstration sites located in six different European countries. These sites vary in history, environmental conditions, and design. In this report, we analyzed 11 of these sites: 8 are dune-in-front-of-dike, one is dune-in-dike, one is dune only, and one is dike-in-dune. Among them, 8 sites involved sand nourishment, 4 had fences, and 8 were planted with marram grass (*Ammophila arenaria*). About half of the sites were established in the past five years.

The aim of this report (**D5.1**) is to evaluate coastal dune habitats according to the **Natura 2000** framework. Annex I of this framework outlines priority habitats designated as special conservation areas by EU countries. Identifying these habitats and monitoring their change over time is essential to ensure their protection.

To cartography those habitats, we curated a set of aerial imagery and elevation data provided by other DuneFront partners and work packages, or publicly available. Based on these, we developed a new classification model for sandy coastal habitat in **Baltic** and **Atlantic geographic regions**. This model helps classifying dune areas into three main types: **embryonic dunes**, **blond dunes**, and **grey dunes**. A temporal analysis was carried out to compare habitat conditions before and after the installation of the demonstration projects, depending on available data. We focus on 11 out of 13 demonstrators, one site lacked sufficient data, and another—the only one located in the Mediterranean—was excluded from the model due to differing habitat types. The results show that the model performs well in identifying embryonic and blond dunes. However, improvements are needed for better detection of grey dune habitats. In most demonstrator sites, the presence of Annex I important habitats increased following the establishment of the site.

DuneFront

Table of Content

DuneFront

List of recurring abbreviations

Abbreviation	Explanation
NbS	Nature-based Solutions
DD-hybrid	Dune-dike hybrid
DEM	Digital Elevation Model
DSM	Digital Surface Model
DTM	Digital Terrain Model
RGB	Red Green Blue
NIR	Near-InfraRed

1. Introduction

1.1 DuneFront Work package 5 overview

1.1.1 General objectives

The overarching goal of Work Package (WP) 5, named "Demonstrator biodiversity", is to use the DuneFront demonstrator sites (**Figure 1.1**), to evaluate the impact of existing dune-dike hybrid (DD-hybrid) Nature-based solutions (NbS) on biodiversity across multiple levels (habitats, species, traits). Specifically, demonstrators will be evaluated for (a) the evolution of Annex I habitats from installation to present, (b) the spatiotemporal organisation of biological diversity across multiple taxa and traits, and (c) the local connectivity and rescue function at local (beach-dune connections) and regional (coastal connectivity across urban zones) scales.

Data from WP5 will support other DuneFront work packages, providing primary data for WP10-12 (focused on assessing plant functional responses, numerical and physical modelling of dune dynamics) and contributing to the development of the DSS-tool and blueprints (WP13-14).

1.1.2 Work Package sub-tasks, milestones and deliverables

WP5 is subdivided into three sub-WPs listed below, each associated with a deliverable:

WP5.1 - Mapping Annex 1 habitat evolution, with D5.1 (August 2025, this report) quantifying each key habitat type and their temporal evolution in each Demonstrator area.

WP5.2 - Biodiversity patterns, with D5.2 (due December 2026) being a comparison of biodiversity between demonstrators and locally matched control areas. These are based on a series of replicated transects across each site, with the same transect design used to evaluate plants, above-ground invertebrates and below-ground biodiversity (the latter using environmental DNA approaches). The successful coordination of this joint sampling design allows for further cross-taxa analyses, and forms **Milestone M5.1**.

WP5.3 - Biodiversity connectivity, with D5.3 (due June 2026) being an evaluation of both local connectivity (e.g. beach to dune) using data from D5.1 and D5.2, as well as regional functional connectivity of key species of conservation interest, combining data from D5.1 with mechanistic connectivity modeling.

Figure 1.1: Location of the 13 European sites used in WP5.1 (the 12 demonstrators in the DuneFront project and an additional site in Ostende, Belgium) (image from https://dunefront.eu/, modified by the authors).

1.2 Goals of WP5.1

The stated goal of WP5.1 is to evaluate the evolution of key dune habitats, as defined in the Annex I of the EU Habitats directive (Directorate-General for Environment, European

Commission, 2013; Bensettiti et al., 2004), in DuneFront demonstrators. Given the focus of the DuneFront project on the interplay between biodiversity and coastal protection, WP5.1 primarily deals with embryonic (habitat code 2110) and blond/white dunes (habitat code 2120), which are the dune habitats most directly relevant to the coastal protection function (e.g. van Puijenbroek et al., 2017). Nonetheless, there is interest in assessing the broader dune succession, from driftline vegetation (habitat code 1210) to the potential transition from blond/white dunes to later successional dune stages (**Figure 1.2**). In this report, we therefore also attempt to map stabilised dunes (further referred to as 2130 although they may also include other vegetated habitat types, 2140 and so on).

This can be divided into four steps:

- (a) **Collate, curate and pre-process relevant aerial images and Digital Elevation Models** (DEM) from DuneFront partners or publicly available repositories

- (b) **Determine habitat ground truth** for reference zones, combining on-site experience during demonstrator visits for WP5.2 (and the associated plant occurrence data), as well as evaluation of publicly available ground-level imagery (e.g. Google Street View, Bell et al., 2022).

- (c) **Develop and critically evaluate a pipeline for habitat classification**, using (a) and (b)

- (d) use the resulting classification to **quantify and evaluate habitat dynamics in space and time** in the demonstrator areas, across several landscape metrics (Hesselbarth et al., 2019).

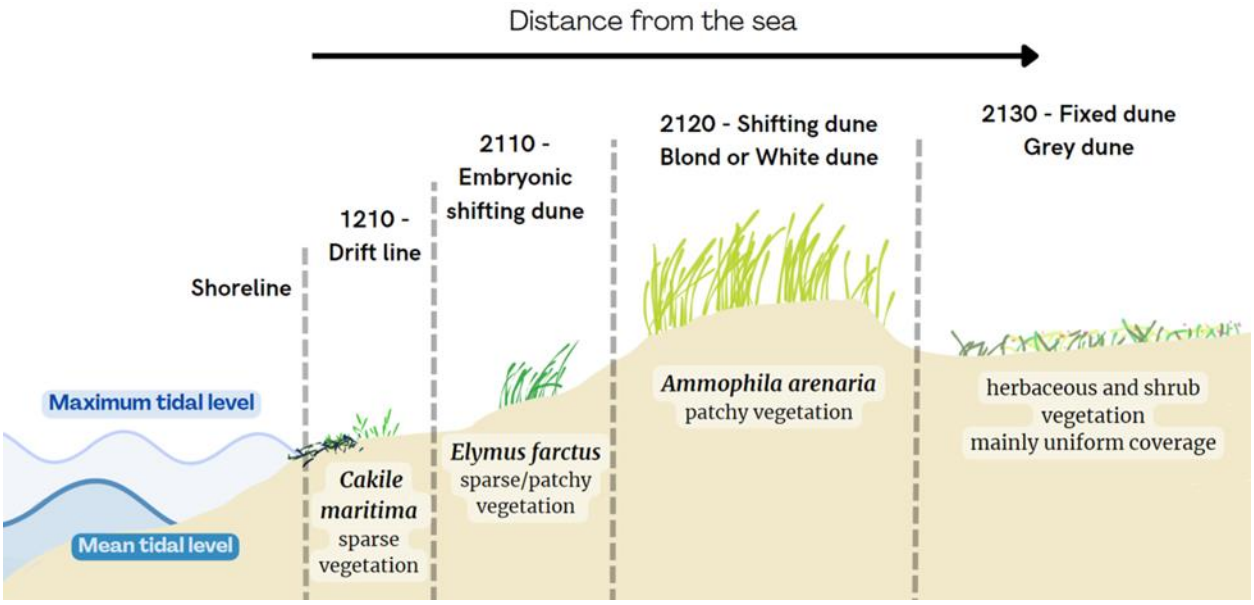

Figure 1.2: Simplified representation of the cross-shore succession of dune habitats on European (Atlantic-Baltic) sandy coasts (credit: Orane Mordacq). See Table 1.1 for a definition of these habitats. The inclusion of the "Drift Line" habitat is planned for future model development but is not covered in this report.

Table 1.1 - Coastal dune habitat studied (Directorate-General for Environment, European Commission, 2013; Bensettiti et al., 2004). The grey dune habitat is a highly variable habitat across Europe defined by several sub-types and species not detailed in this table.

Habitat	Description	Species mentioned in habitat description
1210 Annual vegetation of drift lines	Formations of annuals or representatives of annuals and perennials, occupying accumulations of drift material and gravel rich in nitrogenous organic matter (*Cakiletea maritimae* p.).	*Salsola kali, Atriplex glabriuscula, Cakile maritima, Elymus repens, Eryngium maritimum, Euphorbia paralias, Euphorbia peplis, Glaucium flavum, Matthiola tricuspidata*
2110 Embryonic shifting dunes	Formation of the coasts of the Atlantic, the North Sea, the Baltic Sea and the Mediterranean, representing the first stages of dune construction, constituted by ripples or raised sand surfaces of the upper beach or by a seaward fringe at the foot of the tall dunes.	*Agropyron junceum, Anthemis maritima, Anthemis tomentosa, Elymus fractus, Eryngium maritimum, Euphorbia peplis, Honkenya peploides, Leymus arenarius, Medicago marina*
2120 Shifting dunes along the shoreline with *Ammophila arenaria* ('white dunes')	Mobile dunes forming the seaward cordon or cordons of dune systems of the coasts of the North Sea, the Baltic, and the Atlantic, the Mediterranean. *Ammophilion arenariae, Zygophyllion fontanesii*.	*Ammophila arenaria, Androcymbium psammophilum, Anthemis maritima, Convolvulus caput-medusae, Cutandia maritima, Cyperus capitatus, Echinophora spinosa, Eryngium maritimum, Euphorbia paralias*
2130 Fixed coastal dunes with herbaceous	Fixed dunes stabilised and colonised by more or less closed perennial grasslands and abundant carpets of lichens and mosses, from the Atlantic coasts (and the English Channel) between the Straits of	*Ephedra distachya, Anacamptis pyramidalis, Artemisia campestris, Bromus hordeaceus, Carex arenaria, Corynephorus canescens,*

vegetation ('grey dunes')	Gibraltar and Cap Blanc Nez, and the shores of the North Sea and the Baltic.	*Crucianella maritima, Galium verum, Gentiana campestris*

2. Dataset collection and processing

Data processing was mainly conducted using R4.1.2 (R Core Team, 2021), with QGIS 3.22.4 (QGIS Development Team, 2022) used for map visualization.

2.1 Dataset overview

2.1.1 Study domain

The 'Demonstrator sites' of the DuneFront project span six countries along the European Union coast (**Figure 1.1**). These demonstrators can differ in both social and environmental conditions, as well as in their implementation types (e.g., dune plantations or not; with or without fences). They can be classified into two biogeographical regions: Atlantic-Baltic and Mediterranean. The Perpignan/ Ste-Marie la Mer demonstrator (France) is the only one falling within the Mediterranean biogeographical region. Mediterranean dunes have very different dynamics and biodiversity than Atlantic-Baltic ones (Marcenò et al., 2018), and Mediterranean fixed dunes form a different Natura 2000 category than Atlantic-Baltic fixed dunes (2210 and other 22xx vs. 2130 and other 21xx; Directorate-General for Environment, European Commission, 2013; Bensettiti et al., 2004). After preliminary tests to evaluate to which extent this limited representation of Mediterranean sites would be an issue for classification, we decided to exclude Perpignan data from our general modelling efforts.

We first reached out to DuneFront partners to obtain existing data from their respective demonstrator sites. This approach based on preexisting data leads to variations in the data collected, including differences in spatial and temporal resolutions, as well as in the tools used (e.g., camera types, drone or plane, available wavelengths, calibration, and/or corrections). However, the minimum requirement for inclusion in the global dataset is to obtain spatial and spectral data for each location with a minimum temporal gap. This minimum threshold has not been met for the Porto Demonstrator (Portugal) for which suitable spectral data were unavailable; we therefore excluded this site for further analyses. This results in a total of 11 sites analysed in the present report (**Table 2.1**).

Table 2.1 - Overview of the characteristics of the demonstrator sites used in this report.

Name	Type	Demonstrator installed in (year)	Temporal coverage	Survey frequency	# of surveys after installation	Sand nourishment	Fences	Marram grass planting

Delflandse kust	Dune	2011	1996-2024	Yearly	7	Yes	No	No
Dunkerque	Dune-in-front-of-dike	2020	2019-2023	Twice a year	8	Yes	No	Yes
Fort Napoleon	Dune-in-front-of-dike	2021	2013-2024	Twice a year	5	No	Yes	Yes
Hondsbossche	Dune-in-front-of-dike	2015	1996-2024	Yearly	7	Yes	No	Yes
Katwijk	Dune-on-dike	2015	1996-2024	Yearly	7	Yes	No	Yes
Middelkerke	Dune-in-front-of-dike	2020	2013-2024	Twice a year	5	Yes	No	Yes
Raversijde	Dune-in-front-of-dike	2020	2013-2024	Twice a year	5	Yes	Yes	Yes
Sankt Peter Ording	Dune-in-front-of-old dike	1985	1996-2022	Yearly	4	No	No	No
Soulac	Dune-in-front-of-dike	2024	2012-2024	Twice a year	2	No	Yes	Yes
Texel	Dike-in-dune	2019	1996-2024	Yearly	3	Yes	No	Yes
Ystad	Dune-in-front-of-dike	2011	2002-2022	Each 2 years	6	Yes	Yes	Yes

In addition, to produce a model able to map priority habitats at larger scales than those of the DuneFront demonstrators, data were collected whenever possible, from areas extending beyond the demonstrator's zones. This broader dataset is valuable for training and testing models outside the specific areas of interest for this deliverable. It also supports the development of more global models that can be applied in other studies, as well as aiding future evaluations of habitat differences between the DD-hybrid-NbS Demonstrator system and more natural systems nearby.

The global dataset includes the following areas:

- A larger zone in the Netherlands (with the full Dutch coastline available online; we used approx. 68 km of coasts) available on https://geotiles.citg.tudelft.nl/ [as of February 2025].
- The entire Belgian coast (approx. 67.55 km of coasts) available on https://download.vlaanderen.be/ [as of December 2024].
- An extended area in France around the Soulac demonstrator, stretching from the south of Soulac to the mouth of the Garonne River (approx. 6.51 km of coasts), available on https://www.pigma.org/portail/fr/ [as of 08 January 2025].

However, for the purposes of this deliverable, we will present in **Section 4** only the classification outputs related to the DuneFront demonstrator areas as delimited in Robin et al. (2025).

2.1.2 Curation and preprocessing of source datasets

To conduct a consistent and comparable analysis of Annex I habitat changes over time across all sites, a methodological approach based on raster multispectral imagery has been proposed. This approach utilizes spectral images (acquired through drone or aerial surveys) and elevation data (derived from LiDAR or photogrammetric analysis), all collected from DuneFront partners or publicly available repositories. Additional data on coastal orientation, at about 200-300m resolution, was taken from DuneFront deliverable D4.1 (Castelle & Dahirel, 2024), while the delineation of the demonstrator dunes has been sourced from DuneFront deliverable D6.1 (Robin et al., 2025), or created *de novo* where it was missing (Ostende – Fort Napoleon; Soulac; Dunkerque; Zand Motor – Delftlandse Kust).

Spectral and elevation images collected for each location were classified, renamed, and reorganized. We chose the European Terrestrial Reference System 89 (ETRS89) as a unique coordinate reference system (CRS), and all images were reprojected accordingly. Spectral data were stored as 8-bit images (ranging from 0 to 255 without decimals), while elevation data were stored as float32 (keeping decimals). All images were compressed using DEFLATE (a lossless compression format).

Spectral and elevation images taken within close temporal proximity (preferentially within ±1 year) were considered compatible and merged into a single file. The details of the merging process can be found in Appendix **table A.2.** Each combined file (spectral and elevation data) was then divided into 500 m² plots to facilitate subsequent analysis.

For the purposes of this deliverable, we have chosen to use a single model and, accordingly, only retained common variables across all sites (specifically red, green, blue channels, and elevation, to the exclusion of near infrared, which was only present in some sites). In addition to the data discrepancies mentioned earlier (study domain), it is important to note that the specifics of how spectral information is encoded in red, green, and blue channels vary between different manufacturers or, in some cases, even between sensors from the same manufacturer. However, despite the availability of more specific information in certain instances, we have opted to process all the data together without distinguishing between the characteristics of wavelength encoding into channels, resolution, and calibration.

Similarly, depending on data source, the elevation data collected may correspond to a Digital Terrain Model (DTM, which excludes buildings and vegetation), or to a Digital Surface Model (DSM, which includes all visible surface features), and in some cases, the model type is

unspecified. Both types of elevation rasters are used interchangeably in the analysis; however, when a choice had to be made, DTMs were preferred.

2.1.3 Variables

An innovative aspect of this work lies in recognizing that dune habitats are shaped by different ecological engineers, each influencing dune formation in distinct ways (Maun, 2009). While traditional approaches rely primarily on pixel-wise RGB and near-infrared bands to capture spectral phenotypes, our method goes a step further by also mapping extended phenotypes, reflecting the physical modifications ecosystem engineer species imprint on their environment on a wider scale, and accounting for their effect on dune elevation and shape.

The cropped images were manually checked to remove water images, in order to reduce the dataset size and analysis time. For the cropped images, both elevation and several spectral indices were extracted at the pixel level (**Table 2.2**).

Table 2.2 – List of spectral indices extracted from Croft et al. (2014), Lu et al. (2019) and Yuke (2019)

Abbreviation	Formula
BGI	Blue / Green
GCC	Green / (Green + Red + Blue)
Green	Green / Red
NPCI	(Red - Blue) / (Red + Blue)
ExB	1.4 * Blue - Green
ExG	2 * Green - Red – Blue
ExR	1.4*Red - Green
GLI	(2 * Green - Red - Blue) / (2 * Green + Red + Blue)
mGRVI	(Green^2 - Red^2) / (Green^2 + Red^2)
NGRVI	(Green - Red) / (Green +Red)
RGBVI	(Green^2 - Blue * Red) / (Green^2 + Blue * Red)
VARI	(Green - Red) / (Green + Red - Blue)

In addition to pixel-level indices, we adopted a pixel neighborhood approach. This was to minimize the effect of small intra-dune variations between pixels that do not reflect habitat changes. The mean, minimum, maximum, standard deviation, and 95th percentiles of each standard index were extracted for all pixels within a 5-meter radius around each pixel. Further, because dune ecosystems are highly directional and primarily influenced by coastal orientation (Maun, 2009), we derived the same statistics as above for longshore and cross-shore transects, within the same 5-meter range around each pixel. Coastal orientation data

from Castelle & Dahirel (2024) was used to determine the longshore and cross-shore directions. Additional indices were also included, notably through transformations of the red, green, and blue color channels into alternative color spaces. Such transformations could help reduce the effects of light intensity variations between images, by isolating it on a separate channel from colour variation itself.

- LAB: The LAB color space separates luminance (L) from chromaticity (A and B channels), where A represents the green–red axis and B represents the blue–yellow axis, implemented using the grDevices in R (R Core Team, 2021).

- HSV: Hue, Saturation, and Value (HSV) is a cylindrical-coordinate representation of colors based on the RGB model, implemented using the grDevices in R (R Core Team, 2021).

Distance from the sea—both in absolute terms and as a relative measure normalized within each demonstrator—was computed based on the coastline data in Castelle & Dahirel (2024). Because the distance between the shoreline and the beginning of the dune system can vary significantly depending on the location, we normalized distances within each demonstrator using the maximum observed distance in the imagery for that demonstrator. This allowed us to account for local coastal morphology and enable better comparison across sites.

We also included texture indices, using existing R and Python libraries:

- The glcm package (Zvoleff et al., 2014) calculates texture based on the Grey Level Co-occurrence Matrix (GLCM), which measures the spatial distribution of pixel intensities. We used an offset of 5 and extracted the following statistics for both elevation and green channel data: mean, variance, homogeneity, contrast, dissimilarity, entropy, second moment, and correlation.

- RichDEM, Rich Digital Elevation Models (Barnes et al., 2013) is a high-performance terrain analysis library. It was used to derive additional terrain attributes, including slope, aspect (the direction of steepest descent), profile curvature, and planform curvature.

In the second stage, a subset of 247 cropped plots (combined images of 500 m x 500 m) was selected using a 'guided randomness' approach to ensure a well-balanced representation across sites, years, and sampling methods. Within this subset, clusters of indices showing a Pearson correlation coefficient equal to or greater than 0.9 were removed from further analysis, keeping only one variable per such cluster—except for elevation-derived indices and distance from the sea, which were considered essential for our modeling approach (cf. Dormann et al. 2013). Among highly correlated variable groups, we prioritized simpler variables (using less bands), aiming to reduce computational load. When possible, we

consistently selected the same base index (e.g. GCC mean, GCC minimum, GCC maximum) to maintain uniformity across the analysis.

2.2 Model characteristics

The model used is a supervised classification model called Random Forest, implemented with the *ranger* package in R (Wright & Ziegler, 2017). Random Forest is a widely used method in the scientific literature, and more specifically for dune habitat classification (e.g., in Agrillo et al., 2023; Laporte-Fauret et al., 2020; Marzialetti et al., 2019).

Habitat ground truth data was created for reference zones, based on field experience from the lead author's visits to the demonstrators as part of DuneFront WP5.2 (along with associated plant occurrence data). Additionally, publicly available ground-level imagery (e.g., Google Street View, Bell et al., 2022) was evaluated to support the annotation process.

The ground truth data were created using 29 images of 500 m x 500 m, evenly distributed across the sites and selected to be representative. These datasets consist of polygons identifying areas of embryonic dunes, white dunes, grey dunes, as well as other areas categorized under "Other." Data from the areas annotated with ground truth information were randomly split into 80% for training and 20% for testing.

We ultimately selected 86 variables, that can be grouped in 6 categories: colorspace indices (4 variables, e.g. Saturation), standard indices (5 variables, e.g. GCC), texture indices (11 variables, e.g. Profiles), neighborhood indices (27 variables, e.g. mean elevation), transect indices (37 variables, e.g. mean elevation from transect parallel to the coastline), and distance (2 variables, e.g. distance from the sea) (see **table A1** in Appendix 1).

We chose a hierarchical classification approach, as it provided better predictive performance based on confusion matrix comparisons. The hierarchical classification process involves two steps:

- The first step is a binary Random Forest classifier (using the ROSE algorithm to balance class distribution), which separates dune pixels—encompassing the three habitats: embryonic, white (blond), and grey dunes—from all other pixels.
- The second step applies a multi-class model to the pixels previously classified as "Dune" in order to distinguish between the three dune habitat types.

2.3 Landscape temporal analysis

For the temporal analysis, when data were available, we selected one date prior to the demonstrator's implementation and one date after. This analysis was conducted using the *landscapemetrics* R package (Hesselbarth et al., 2019), which calculates landscape metrics by class—in our case, the dune habitats.

We focused on comparing three class-level metrics:

- Aggregation Index (ranges between 0 and 100%): This metric is defined as the number of like adjacencies divided by the theoretical maximum number of like adjacencies for that class. It reflects the degree of spatial clustering within each habitat class. Lower values correspond to more disaggregated, or patchy, habitat.
- Total Area: The total habitat class area sums the absolute area of all patches belonging to a class. It shows if the landscape is e.g. dominated by one class or if all classes are equally present.
- Percentage of Landscape (ranges between 0 and 100%): This metric represents the relative proportion of the area classified as dune occupied by a particular habitat class. It provides insight into the relative dominance or scarcity of a class within the overall landscape. Lower values mean the focal habitat is less represented among the area classified as dune overall; i.e. this metric can change even if the Total Area of all dune classes remains constant. Conversely, the Percentage of Landscape for a focal habitat can stay constant even if its Total Area changes, if the Total Areas of all dune classes see the same proportional changes.

3. Model performance

We used a confusion matrix approach to evaluate the model's performance in correctly identifying the different classes (**Table 3.1** and **Table 3.2**). All performance metrics provided below are on the test data.

The classification model demonstrated strong overall performance, with an accuracy of 96.84% for the binary model than separates dunes from other land covers (mainly trees, sand and water), and 93.69% for the multi-class model. Accuracy represents the proportion of correctly classified instances across all predictions. For the multi-class model, performance varied by class: blond dunes and embryonic dunes were reasonably well identified, with sensitivities of 0.86 and 0.77 respectively. Sensitivity measures how well the model detects the actual instances of a class. Additionally, the specificity for blond and embryonic dunes was above 0.97, which means the model avoided errors by correctly identifying areas with no blond or embryonic dunes. Embryonic dunes classification performed well in our model, particularly knowing that it is a little-represented habitat of small size (less than 2%

prevalence). Prevalence refers to how frequent a class is within the dataset. On the other hand, grey dunes were much harder for the model to detect. With a sensitivity of just 0.34, a lot of grey dunes were missed, even though the model had high precision at 0.92, indicating that the model was highly selective—it fails to identify a large portion of them, resulting in many false negatives. Grey dunes were misclassified as blond dunes or as in non-dune cover in roughly similar proportions. This detection failure could be due to several reasons, such as high variability in grey dune across the dataset, visual similarities with other land types, or the relatively small number of grey dunes in the dataset, making them underrepresented and harder to detect.

This contrast suggests a potential imbalance in feature representation or class prevalence affecting recall. In comparison, the dominant "Other" class was detected with near-perfect performance (sensitivity 0.995, precision 0.97), underscoring the model's bias toward well-represented categories. These results point to the next step in this work: improving the differentiation of minority dune classes, particularly grey dunes, in order to enhance overall ecological mapping accuracy. This remains important even though the focus of this project is mainly on blond-embryonic dune habitats (as NbS hybrid dunes in front of dikes are expected to primarily restore such habitats).

After the model is trained, it is applied to all images from the demonstrator sites, within the dune areas delineated by WP6.1. This serves as a habitat mapping tool to enable temporal comparisons.

Table 3.1 Confusion matrix and statistics for the binary model separating dunes of interest from all other land covers

	Reference	
Prediction	Dune	Other
Dune	99623	3128
Other	22011	671025

Statistics	
Accuracy	0.968
95% CI	(0.968, 0.969)
No Information Rate	0.848
P-Value [Acc > NIR]	< 2.2e-16
Kappa	0.870
Mcnemar's Test P-Value	< 2.2e-16

	Dune
Sensitivity	0.819
Specificity	0.995
Pos. Pred. Value	0.970
Neg. Pred. Value	0.968
Prevalence	0.153
Detection Rate	0.125
Detection Prevalence	0.129
Balanced Accuracy	0.907

Table 3.2 Confusion matrix and statistics for the overall multi-class model

	Reference			
Prediction	Blond dune	Embryonic dune	Grey dune	Other
Blond dune	43851	2169	16616	1676
Embryonic dune	4893	11750	0	1194
Grey dune	1399	0	18945	258
Other	848	1253	19910	671025

Statistics	
Accuracy	0.937
95% CI	(0.936, 0.937)
No Information Rate	0.847
P-Value [Acc > NIR]	< 2.2e-16
Kappa	0.752
Mcnemar's Test P-Value	NA

	Blond dune	Embryonic dune	Grey dune	Other
Sensitivity	0.86	0.77	0.34	0.995
Specificity	0.97	0.99	0.997	0.82
Pos. Pred. Value	0.68	0.66	0.912	0.97
Neg. Pred. Value	0.99	0.996	0.95	0.97
Precision	0.68	0.66	0.92	0.97

F1	0.79	0.72	0.50	0.98
Prevalence	0.06	0.02	0.07	0.85
Detection Rate	0.06	0.01	0.02	0.84
Detection Prevalence	0.08	0.02	0.03	0.88
Balanced Accuracy	0.92	0.88	0.67	0.91

4. Demonstrator cartography and temporal analysis

4.1 Delftlandse kust (The Netherlands)

4.1.1 Area overview

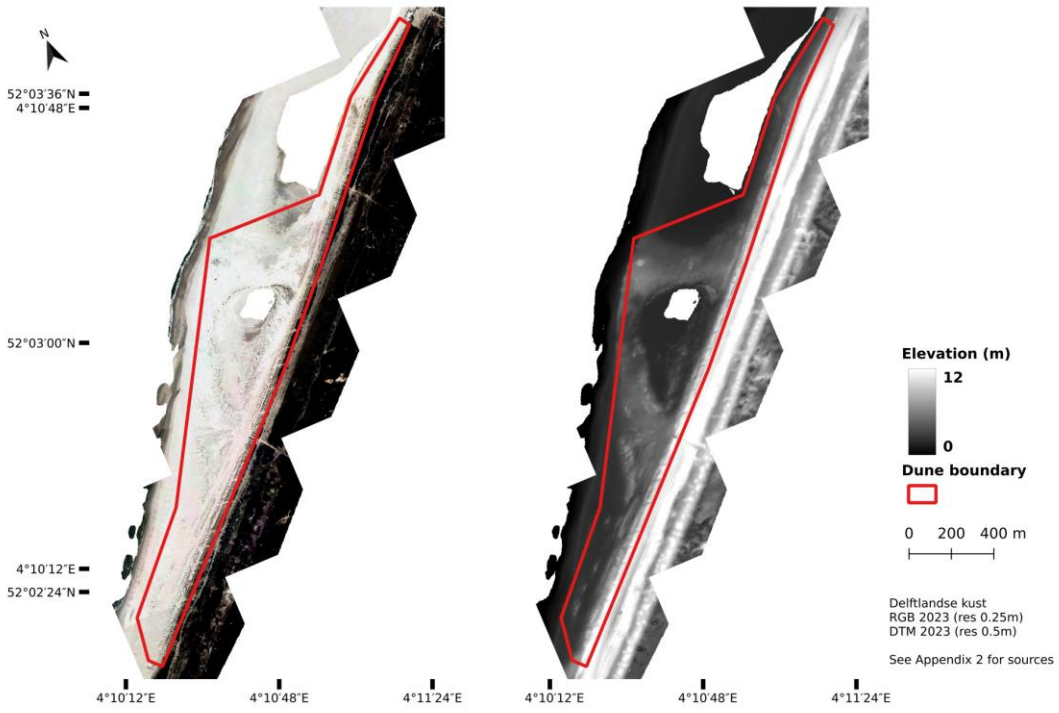

Figure 4.1: Most recent available RGB map (left) and Elevation map (right) for Delftlandse kust.

4.1.2 Habitat cartography

DuneFront

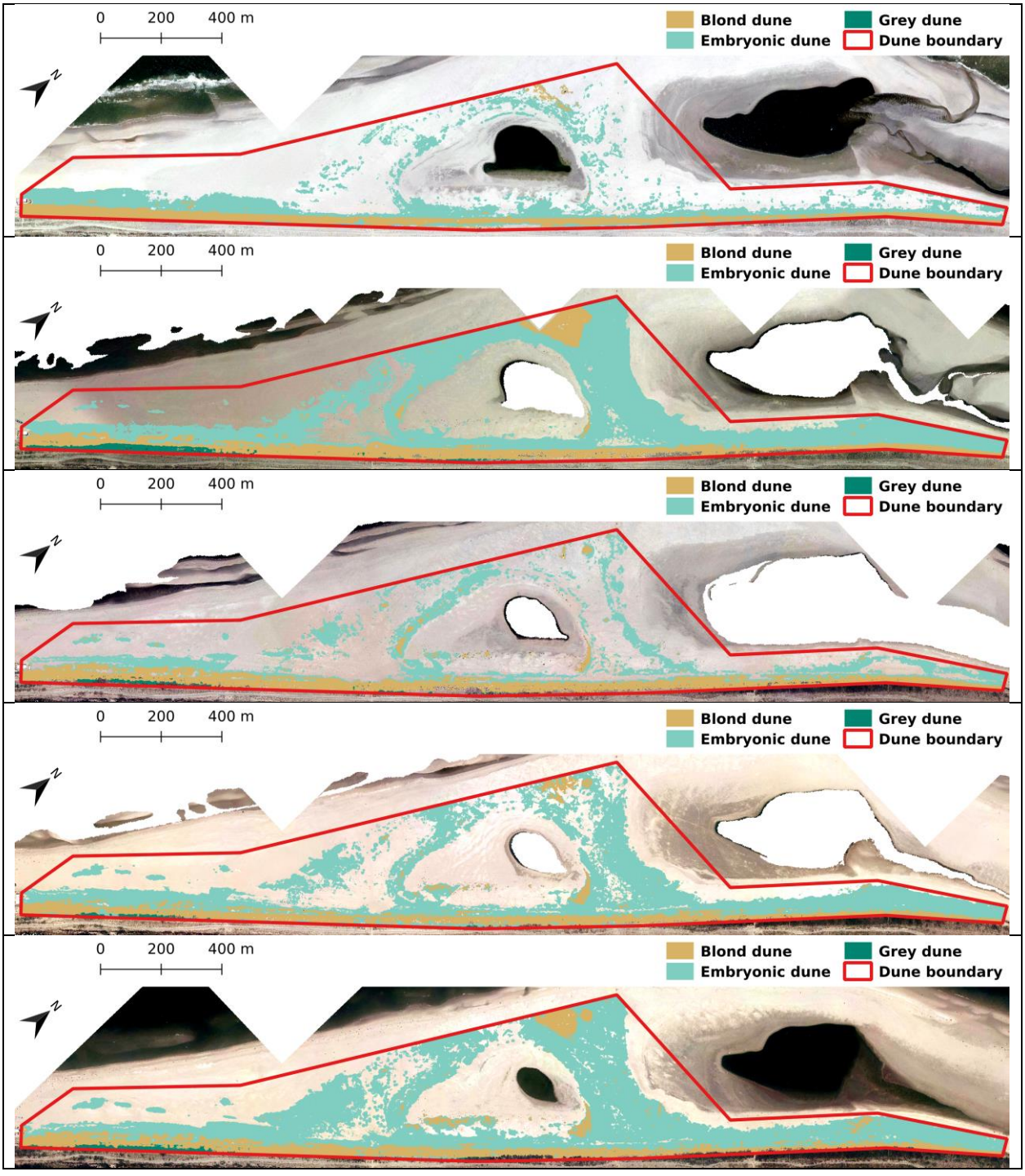
0 200 400 m
Blond dune
Embryonic dune
Grey dune
Dune boundary
N

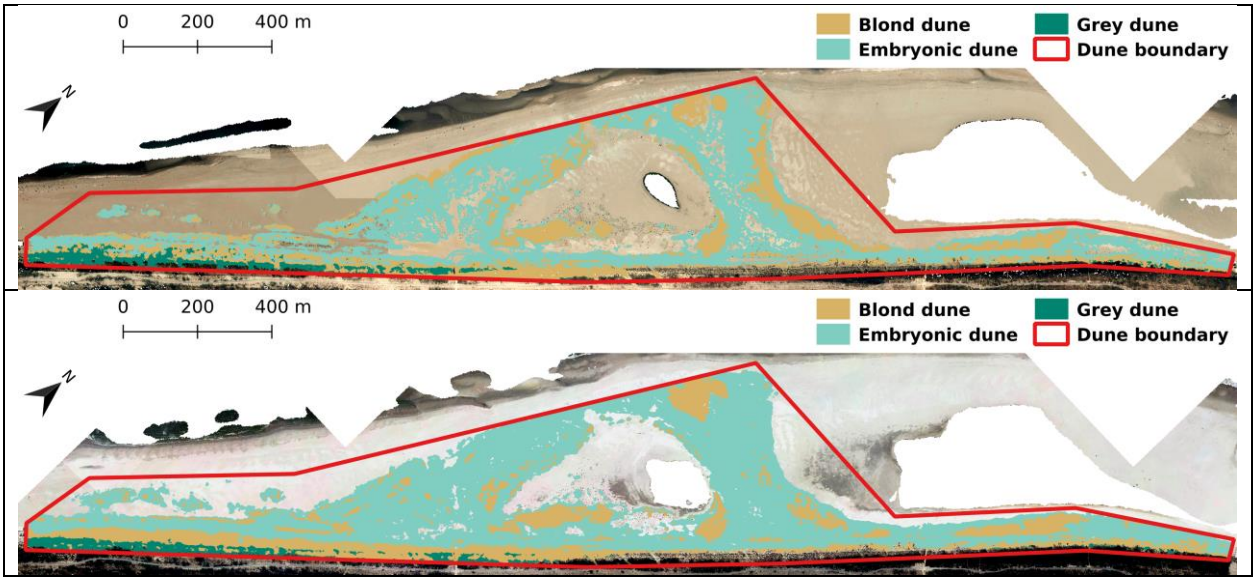

Figure 4.2: RandomForest habitat classification at T1 = 2016, T2 = 2017, T3 = 2018, T4 = 2019, T5 = 2020, T6 = 2022, T7 = 2023 for Delftlandse kust. Classification is overlaid on the corresponding temporal RGB map.

4.1.3 Temporal analysis

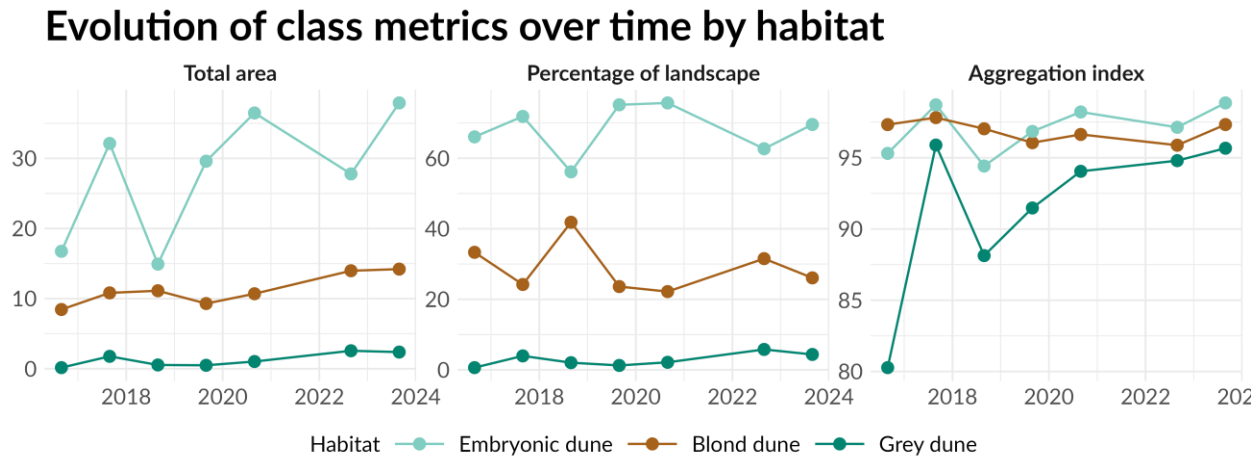

Figure 4.3 Evolution of some landscape metrics in time by habitat for Delftlandse kust.

Disregarding 2017, which shows exceptionally high values compared to previous and following years for embryonic and grey dunes likely due to a classification error, the temporal evolution across the remaining dates reveals a consistent trajectory of dune stabilization. Established in 2011, the site already exhibited a developed dune system at the beginning of the monitoring period in 2016. Blond dunes showed a steady increase in both area and aggregation index, highlighting their expansion and spatial consolidation over time. Grey dunes, although still

limited in extent, exhibited increasing values in area, suggesting a slow but progressive development of late-successional dune stages.

4.2 Dunkerque (France)

4.2.1 Area overview

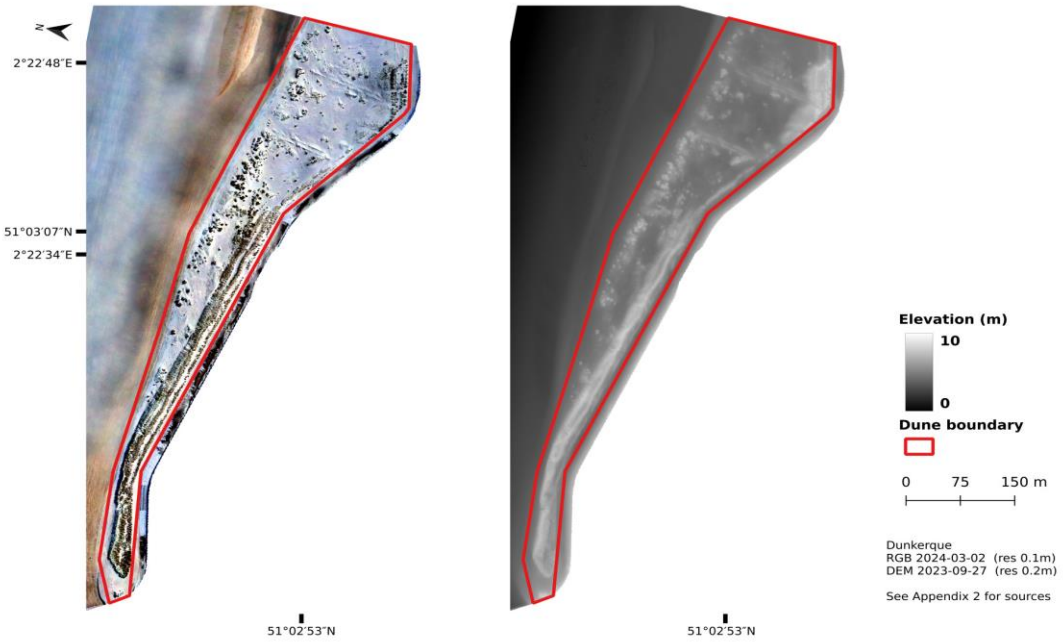

Figure 4.4: Most recent available RGB map (left) and Elevation map (right) for Dunkerque.

4.2.2 Habitat cartography

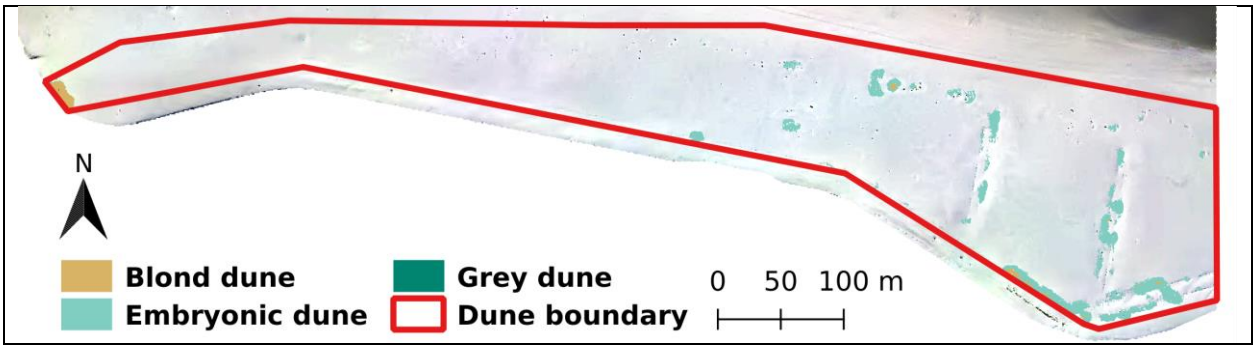

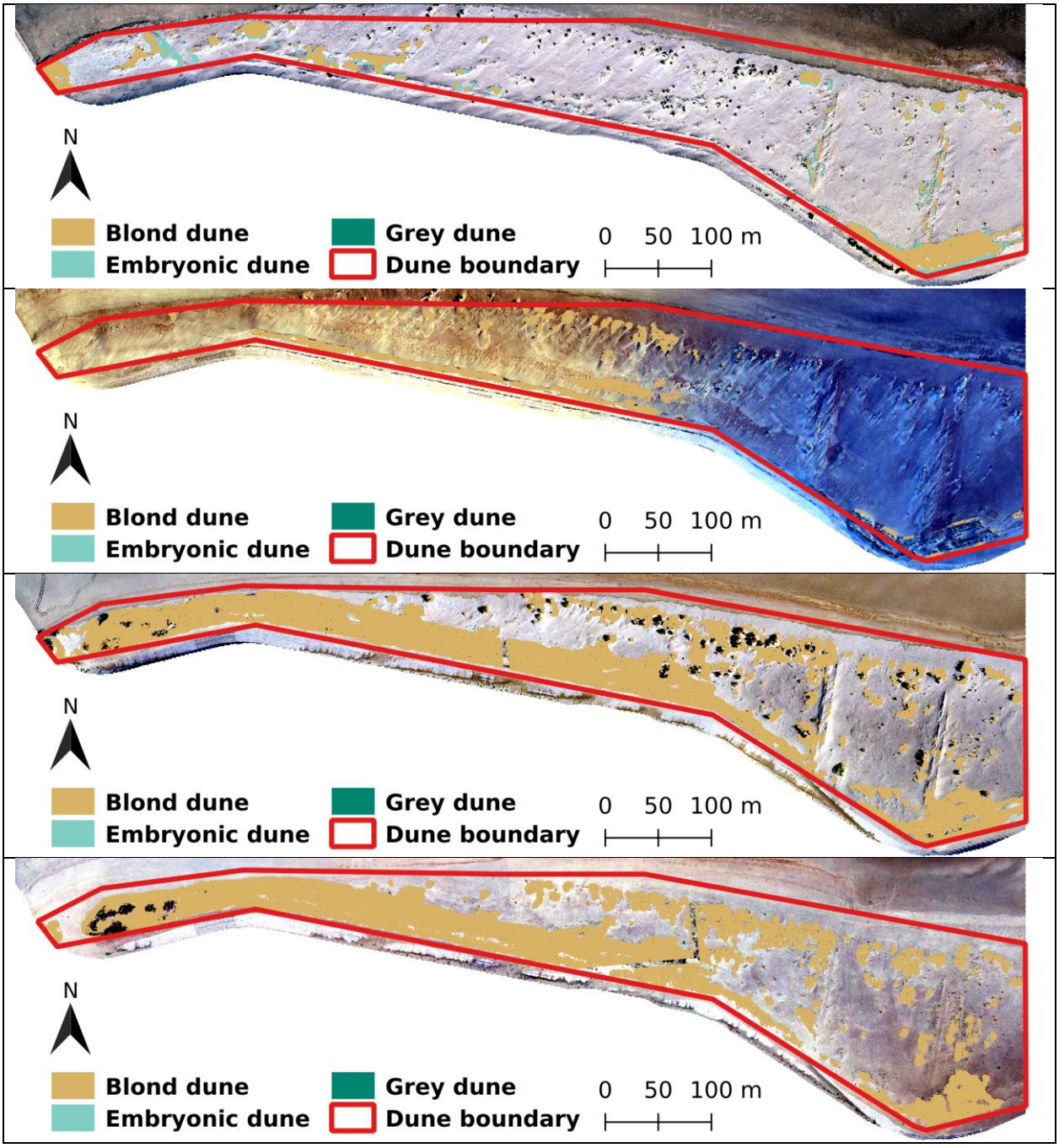
N
Blond dune
Embryonic dune
Grey dune
Dune boundary
0 50 100 m
N
Blond dune
Embryonic dune
Grey dune
Dune boundary
0 50 100 m
N
Blond dune
Embryonic dune
Grey dune
Dune boundary
0 50 100 m
N
Blond dune
Embryonic dune
Grey dune
Dune boundary
0 50 100 m

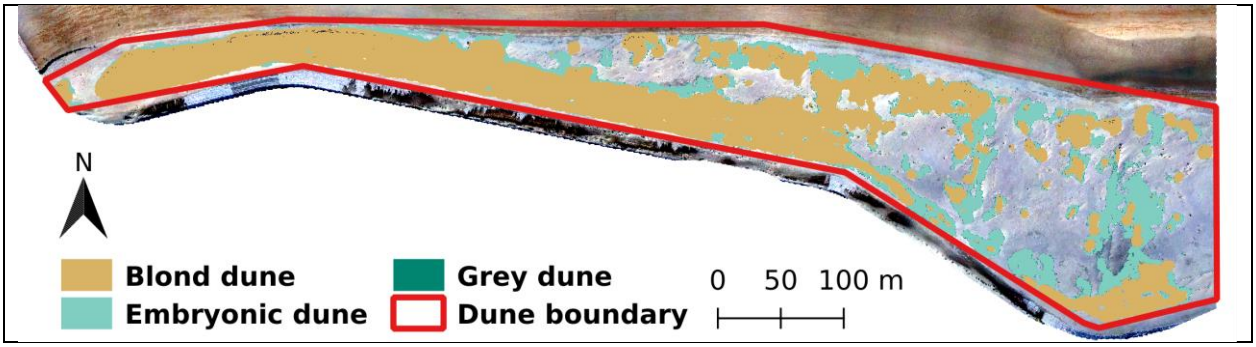

Figure 4.5: RandomForest habitat classification at T1 = 2018-05, T2 = 2020-09, T3 = 2021-04, T4 = 2022-09, T5 = 2023-09, T6 = 2024-03 for Dunkerque. Classification is overlaid on the corresponding temporal RGB map.

4.2.3 Temporal analysis

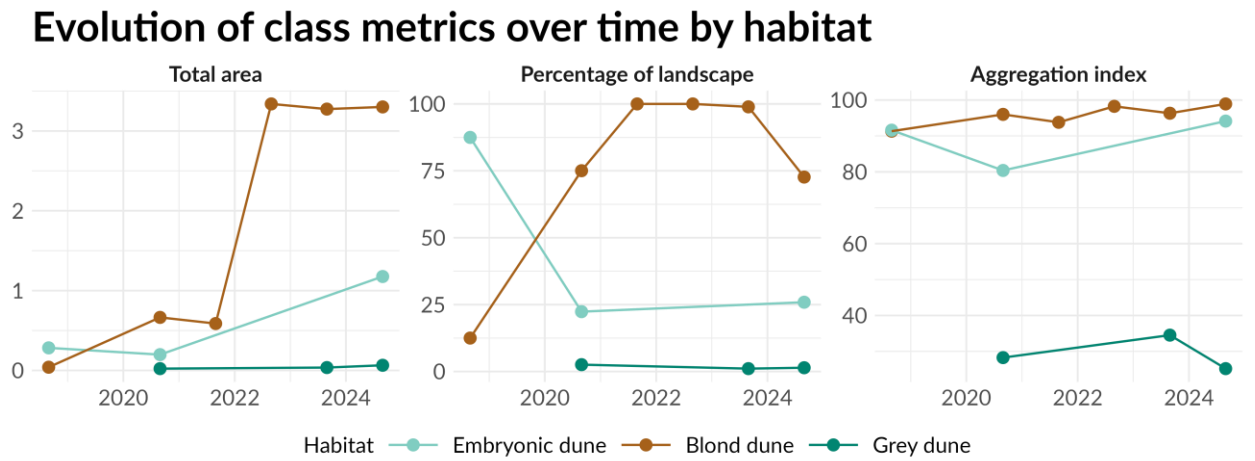

Figure 4.6: Evolution of some landscape metrics in time by habitat for Dunkerque.

Planted in 2020, the blond dune habitat expanded from 0 to over 3 hectares within a few years. It is now the dominant habitat type on the site and has maintained a stable surface area. Prior to the plantation, only a few patches of embryonic dune were present. Recently, the embryonic dune habitat has become more prominent, covering over 1 hectare and accounting for approximately 25% of the total area, which is consistent with field observations from 2024. However, some embryonic dune areas may have been missed in the classifications from 2022 and 2023.

4.3 Fort Napoleon (Belgium)

4.3.1 Area overview

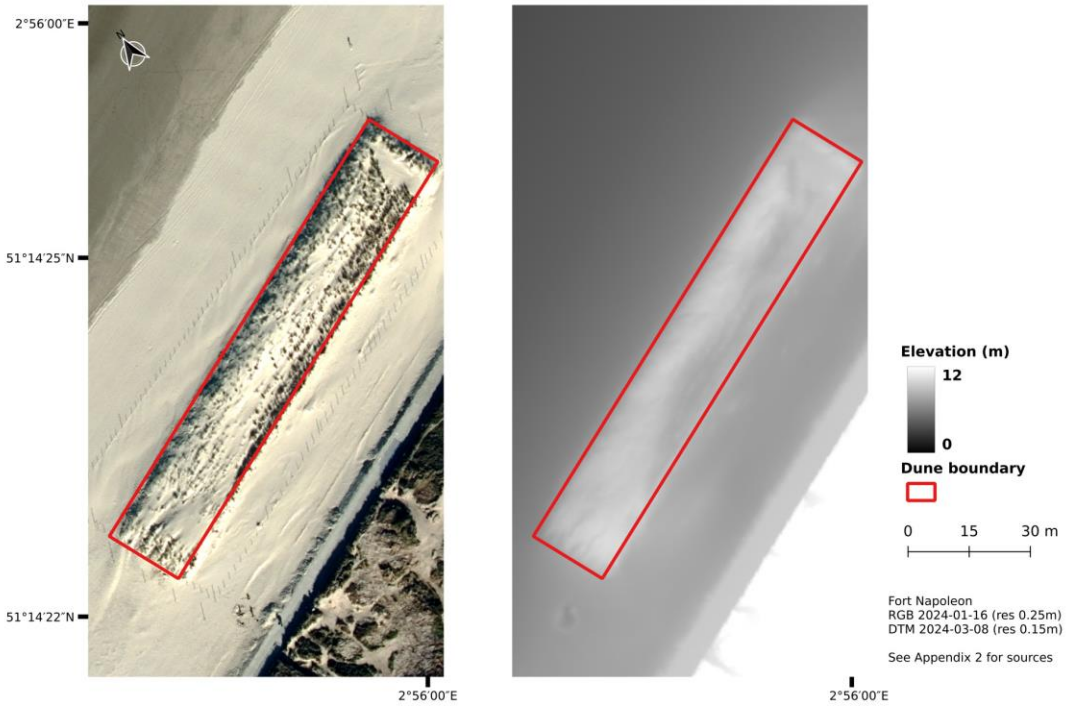

Figure 4.7: Most recent available RGB map (left) and Elevation map (right) for Fort Napoleon.

4.3.2 Habitat cartography

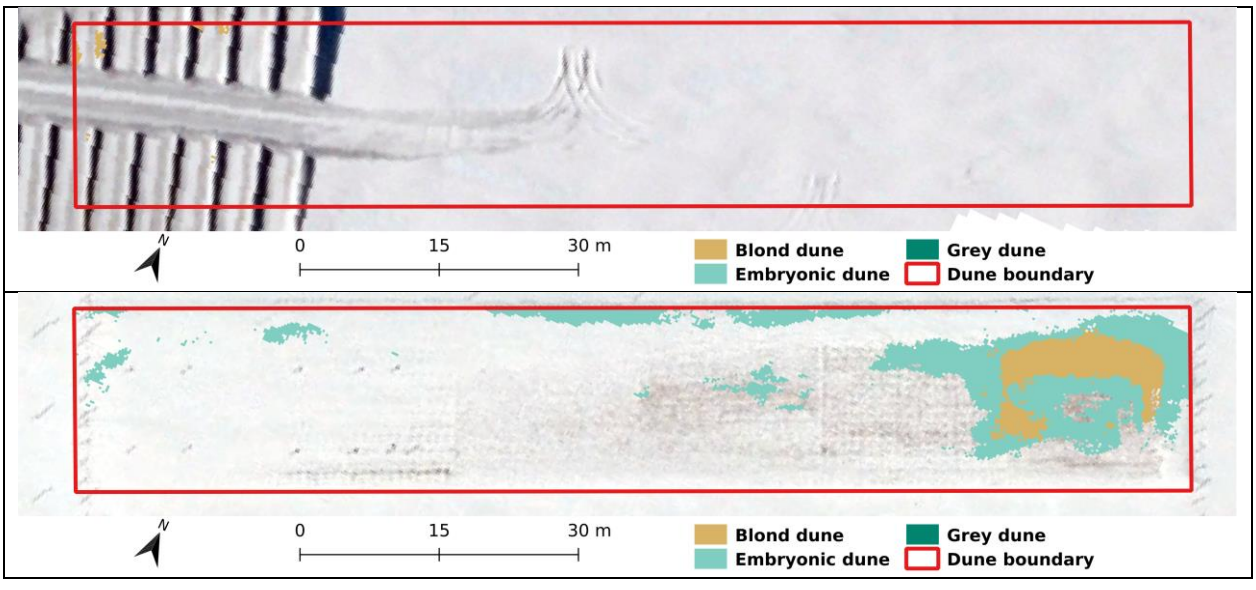

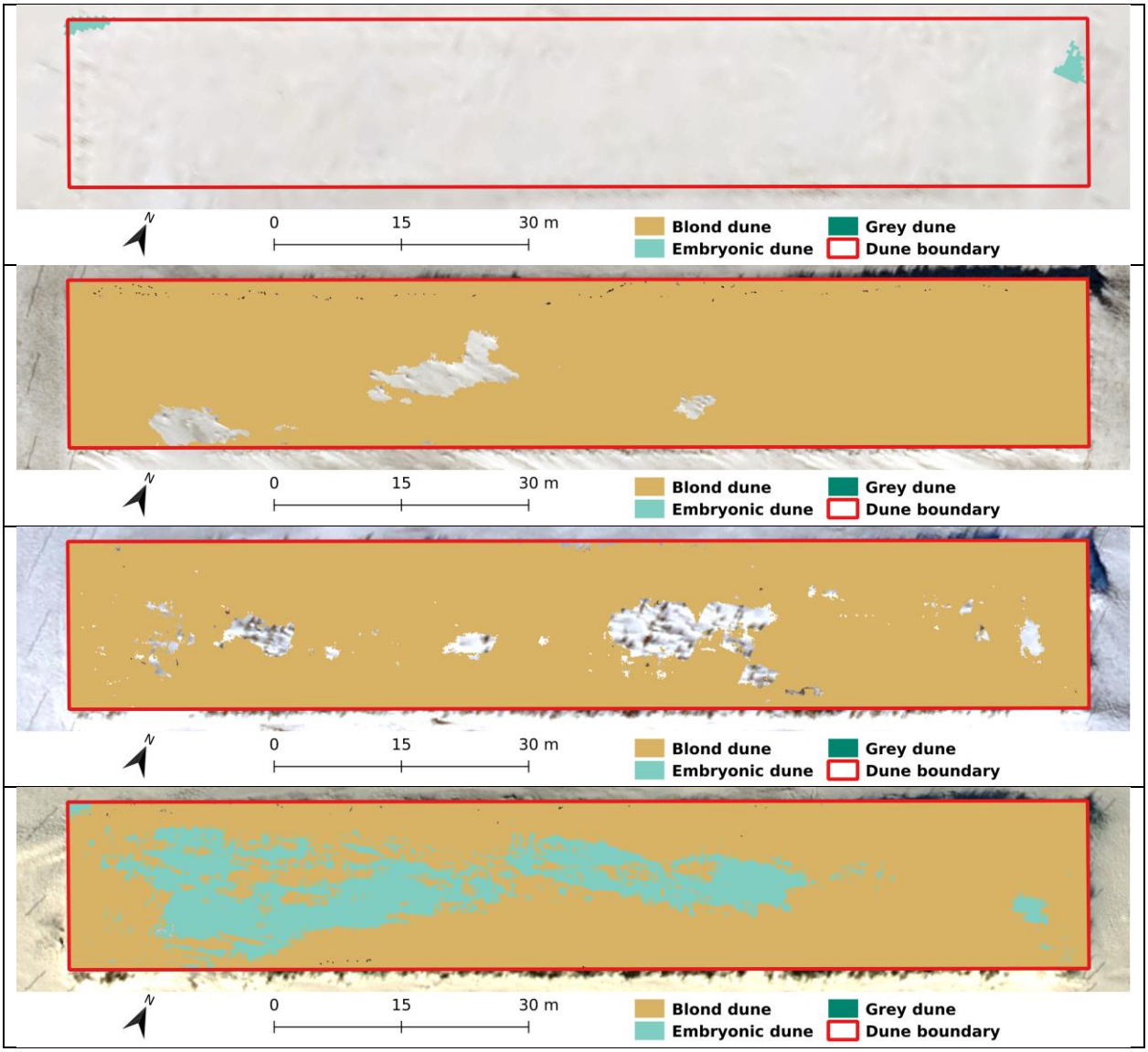

Figure 4.8: RandomForest habitat classification at T1 = 2020-03, T2 = 2021-03, T3 = 2021-07, T4 = 2022-02, T5 = 2023-07, T6 = 2024-03-08 for Fort Napoleon. Classification is overlaid on the corresponding temporal RGB map.

4.3.3 Temporal analysis

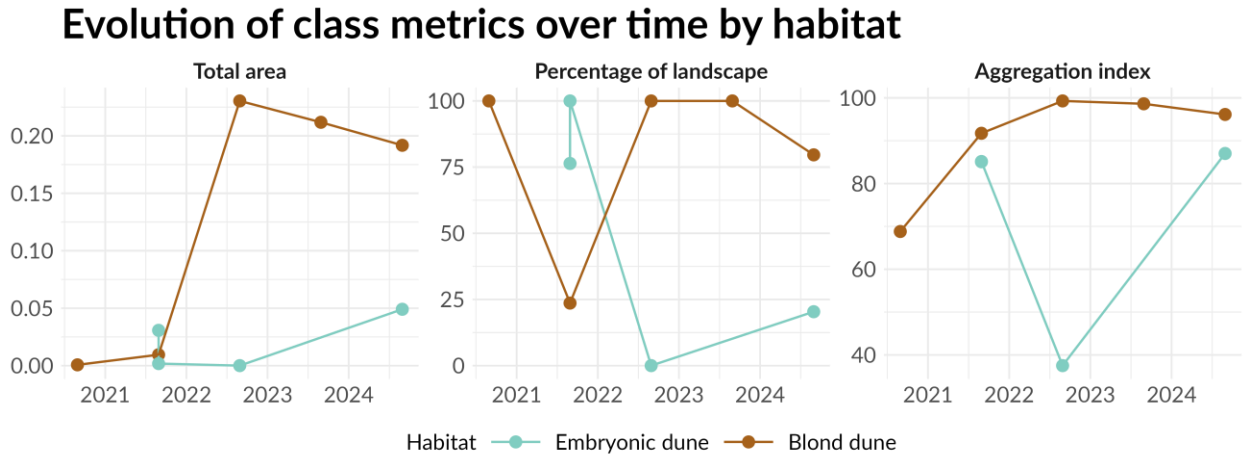

Figure 4.9: Evolution of some landscape metrics in time by habitat for Fort Napoleon.

The temporal evolution of blond dune and embryonic dune reveals marked fluctuations in their spatial extent, aggregation, and dominance within the landscape from 2020 to 2024. Before the plantation in 2020, this area consisted only of sandy beach. In the following spring, the model partially classified the planted area mainly as embryonic dunes, with blond dunes appearing in the center of the plantation and the south-west part already showing signs of burial. However, consistent with the aerial images in Figure 4.8, the planted area was almost completely buried in 2020 summer. Overall, between 2020 and 2024, the blond dune showed a clear increase in area from 0.0007 ha to 0.19 ha and aggregation index improving indicating a more connected and expanded habitat. The embryonic dune displayed more irregular dynamics: its area peaked in 2021 (0.031 ha), dropped sharply in 2022, and recovered to 0.049 ha by 2024. No grey dune was found in this demonstrator, and this is also what was observed in the vegetation survey in 2024.

4.4 Hondsbossche duinen (The Netherlands)

4.4.1 Area overview

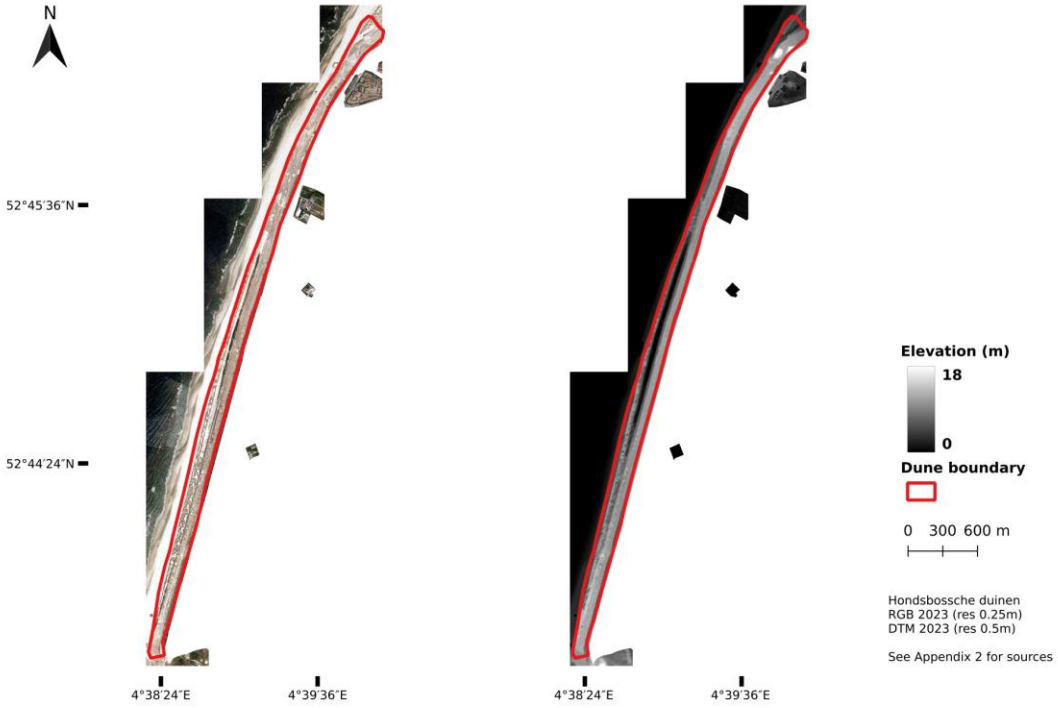

Figure 4.10: Most recent available RGB map (left) and Elevation map (right) for Hondsbossche duinen.

4.4.2 Habitat cartography

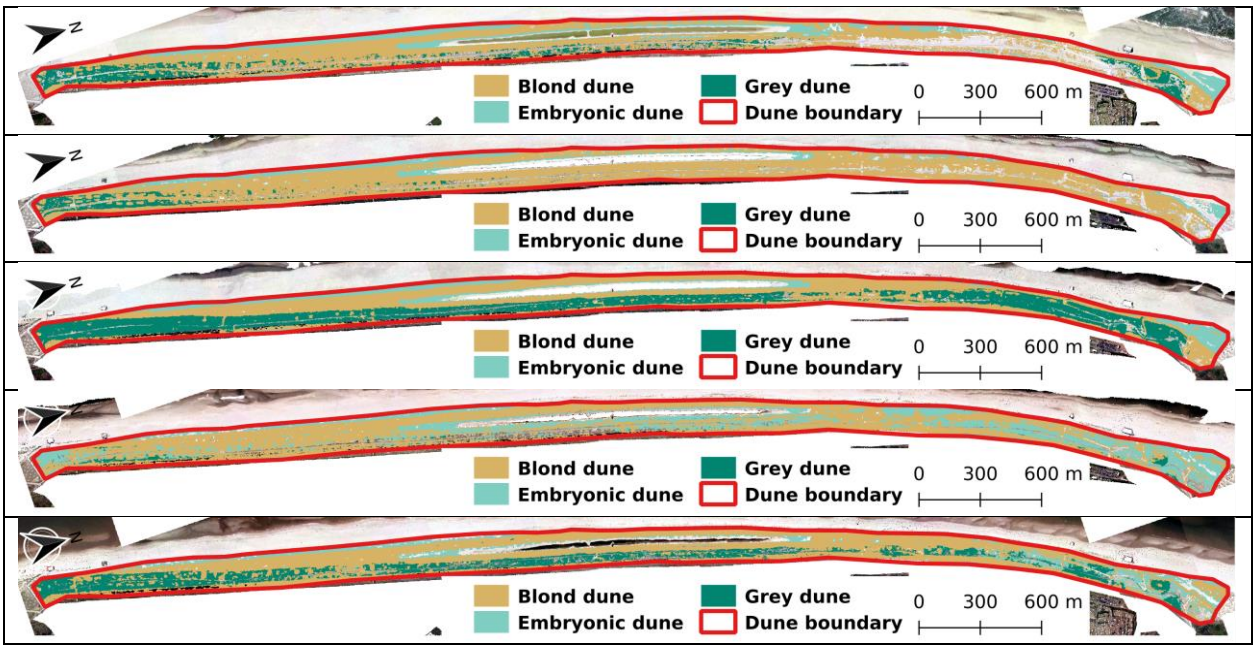

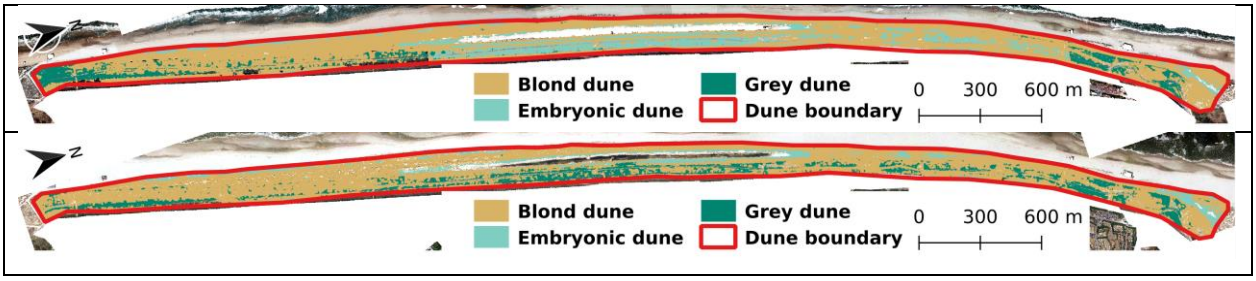

Figure 4.11: RandomForest habitat classification at T1 =2016, T2 = 2017, T3 = 2018, T4 = 2019, T5 = 2020, T6 = 2022, T7 = 2023 for Hondsbossche duinen. Classification is overlaid on the corresponding temporal RGB map.

4.4.3 Temporal analysis

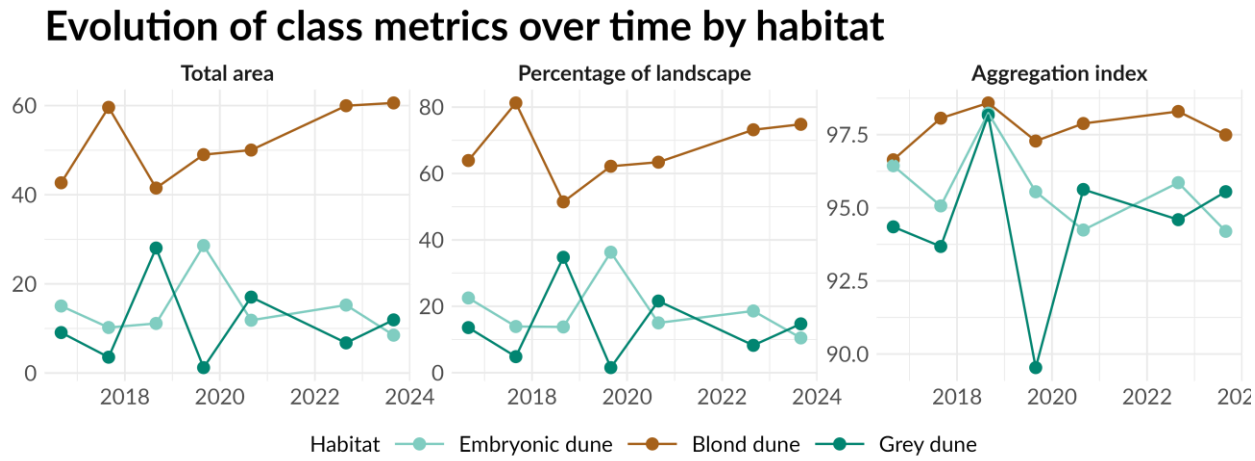

Figure 4.12: Evolution of some landscape metrics in time by habitat for Hondsbossche duinen.

Between 2016 and 2023, blond dunes steadily expanded their surface area, increasing from 63.9% to 74.8% of the landscape, confirming their dominant and growing role in the system. In contrast, embryonic dunes showed a marked decline, shrinking from 22.5% to just 10.5%, indicating significant regression or possible succession toward more mature habitats. Grey dunes exhibited a fluctuating but generally increasing trend, peaking at over 34% in 2018 before stabilizing between 14% and 21% in recent years. However, the sharp variations observed—particularly between 2018 and 2019 —may partly reflect classification errors, as grey dunes are known to be more difficult to distinguish reliably.

4.5 Katwijk (The Netherlands)

4.5.1 Area overview

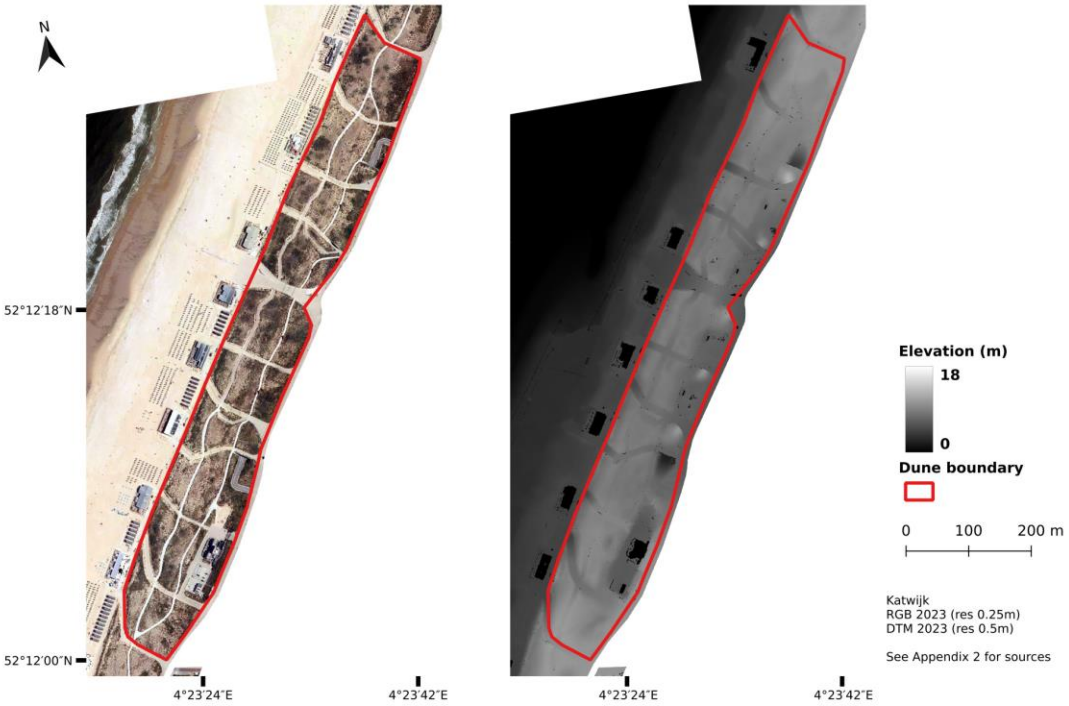

Figure 4.13: Most recent available RGB map (left) and Elevation map (right) for Katwijk.

4.5.2 Habitat cartography

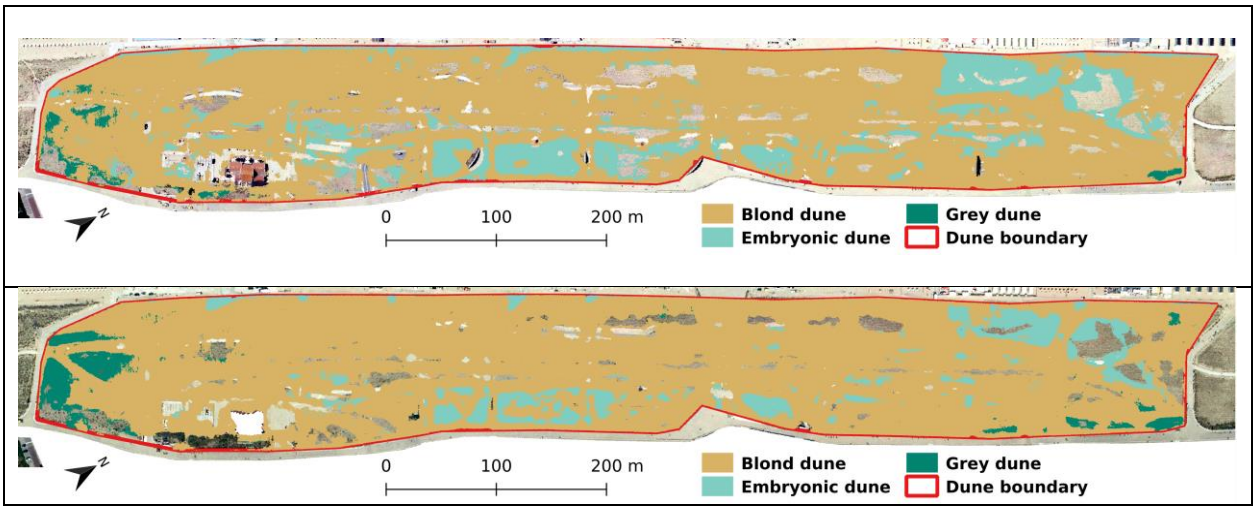

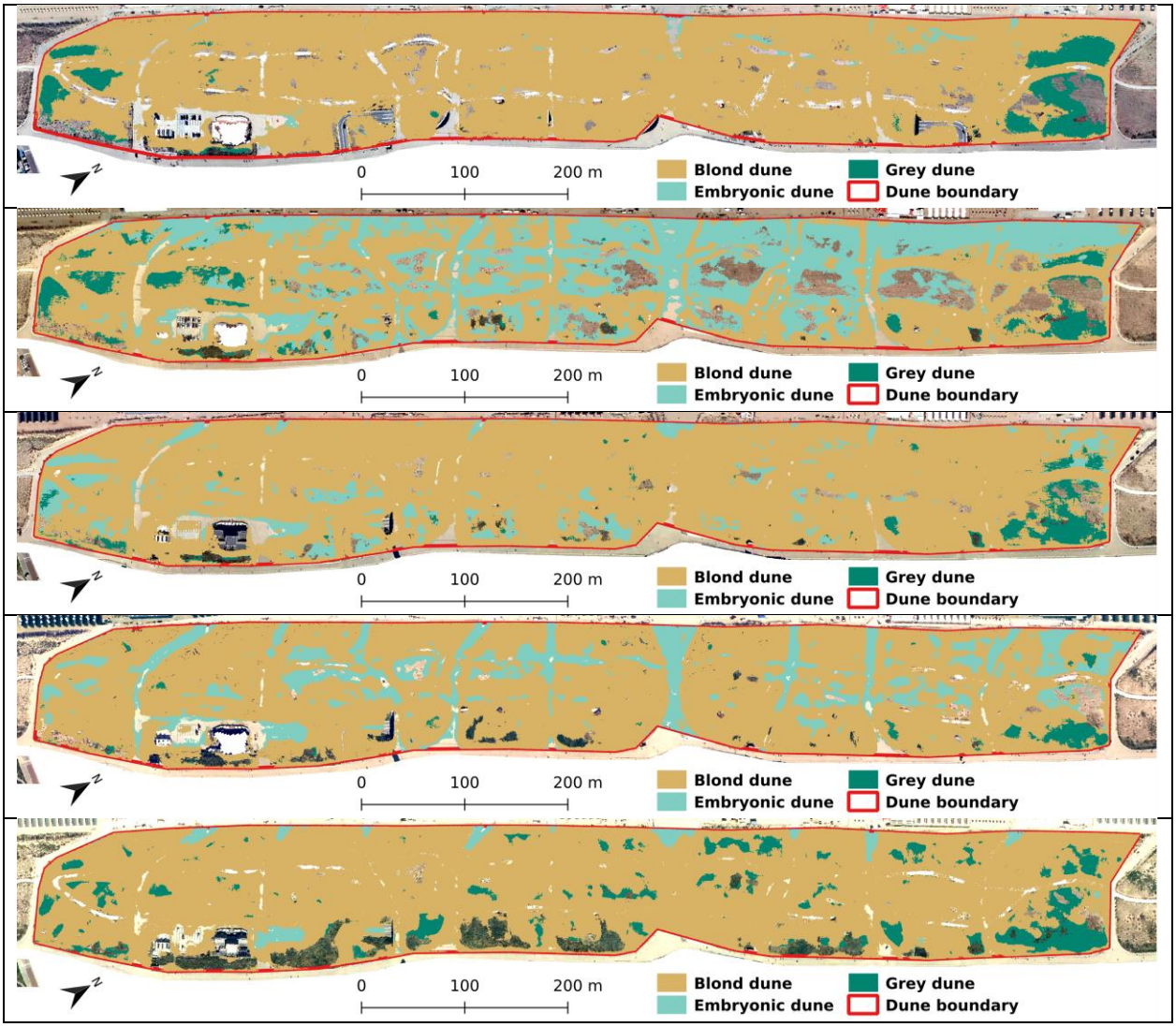

Figure 4.14: RandomForest habitat classification at T1 = 2016, T2 = 2017, T3 = 2018, T4 = 2019, T5 = 2020, T6 = 2022, T7 = 2023 for Katwijk. Classification is overlaid on the corresponding temporal RGB map.

4.5.3 Temporal analysis

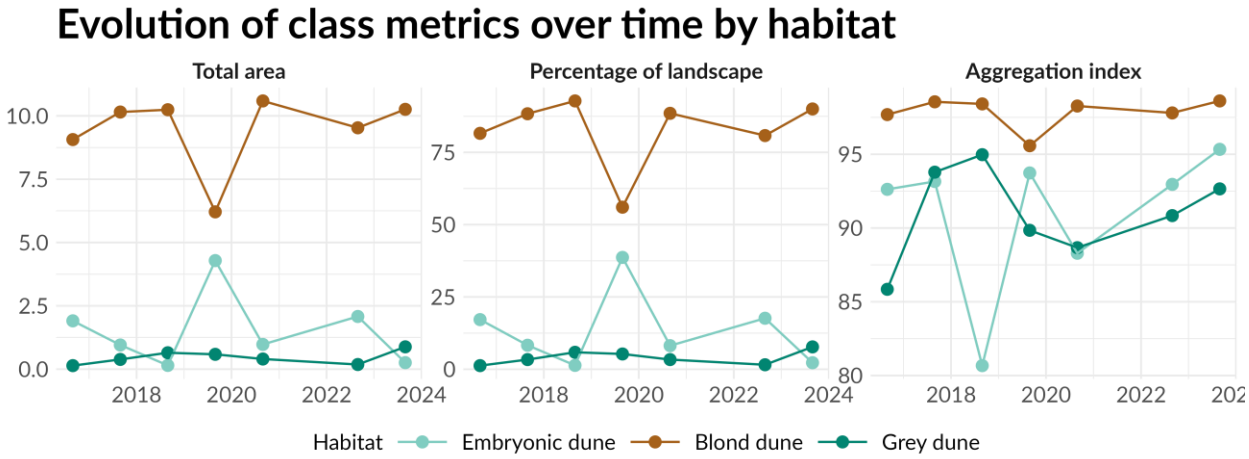

Figure 4.15: RandomForest habitat classification for Katwijk.

Between 2016 and 2023, blond dunes remained stable, with consistently high connectivity (AI > 95%) and dominant surface coverage. Embryonic dunes exhibited a very limited presence with high variability, with major losses in surface area in 2018 and again after 2019, reflecting their sensitivity to disturbance. Grey dunes progressively expanded in area, indicating a slow but steady stabilization or recovery trend. This spatial distribution aligns well with field observations: little to no embryonic dune, a large extent of blond dune, and the progressive formation of grey dune areas.

4.6 Middelkerke (Belgium)

4.6.1 Area overview

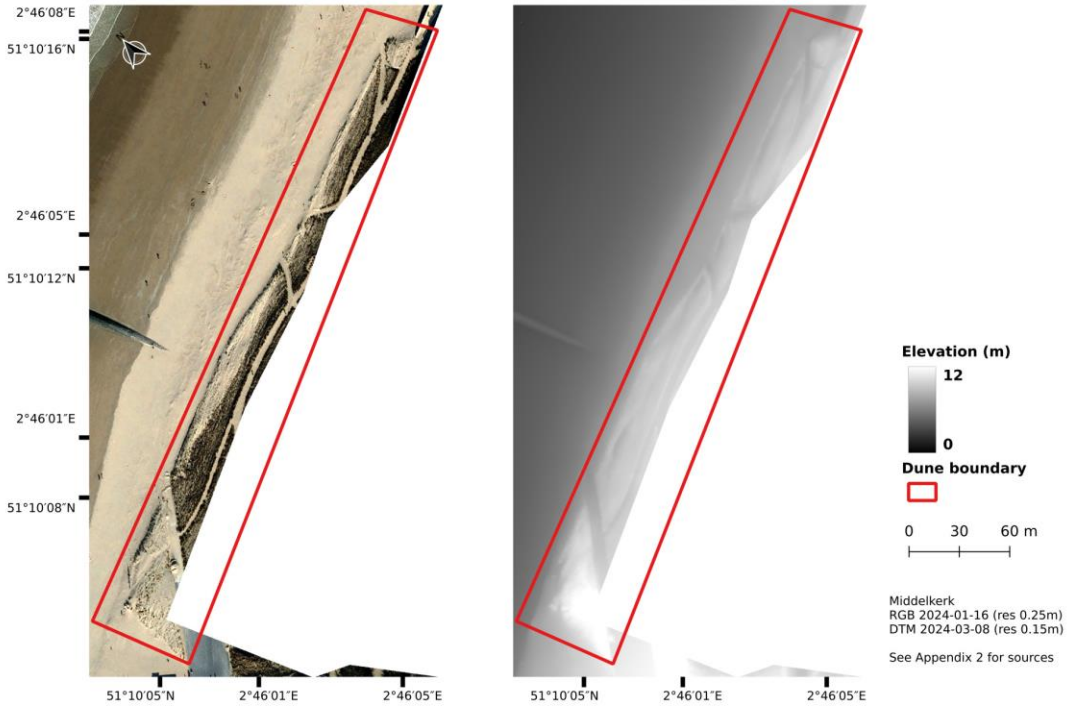

Figure 4.16: Most recent available RGB map (left) and Elevation map (right) for Middelkerke.

4.6.2 Habitat cartography

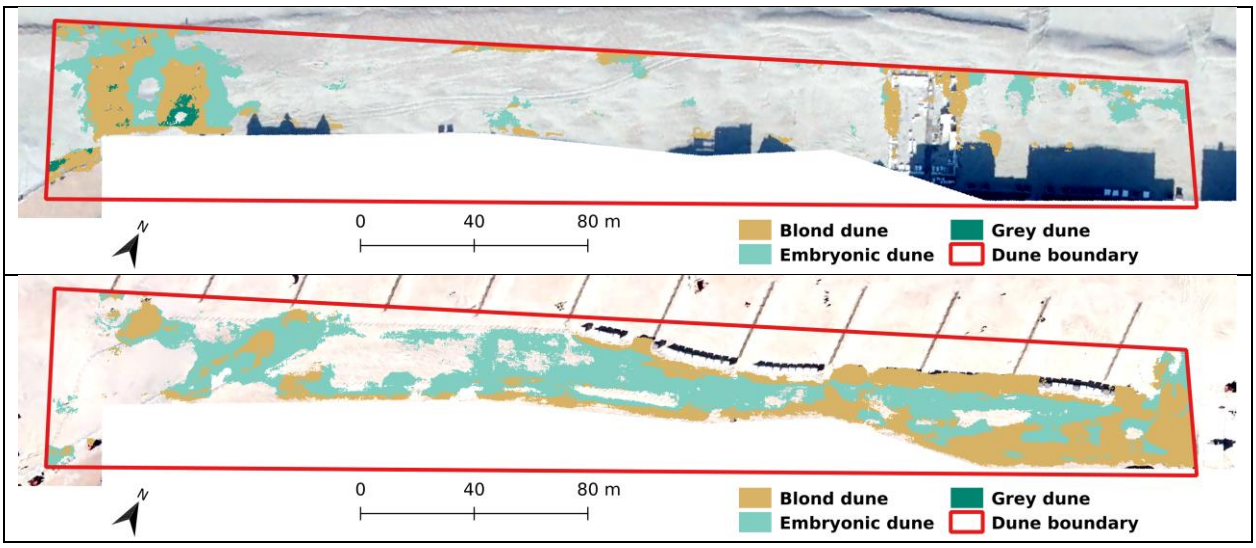

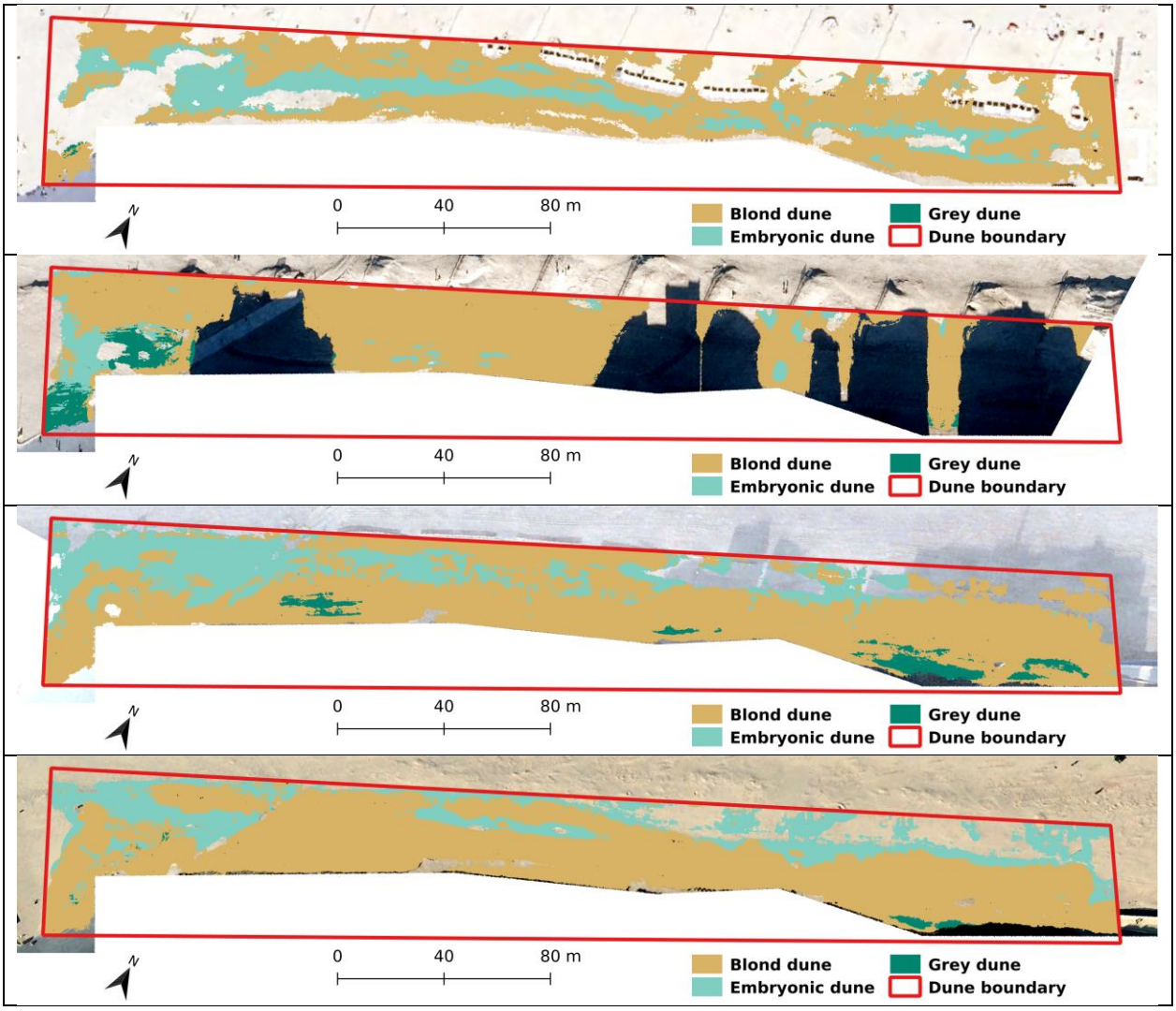

Figure 4.17: RandomForest habitat classification at T1 = 2020-03, T2 = 2021-03, T3 = 2021-07, T4 = 2022-02, T5 = 2023-07, T6 = 2024-03-08 for Middelkerke. Classification is overlaid on the corresponding temporal RGB map

4.6.3 Temporal analysis

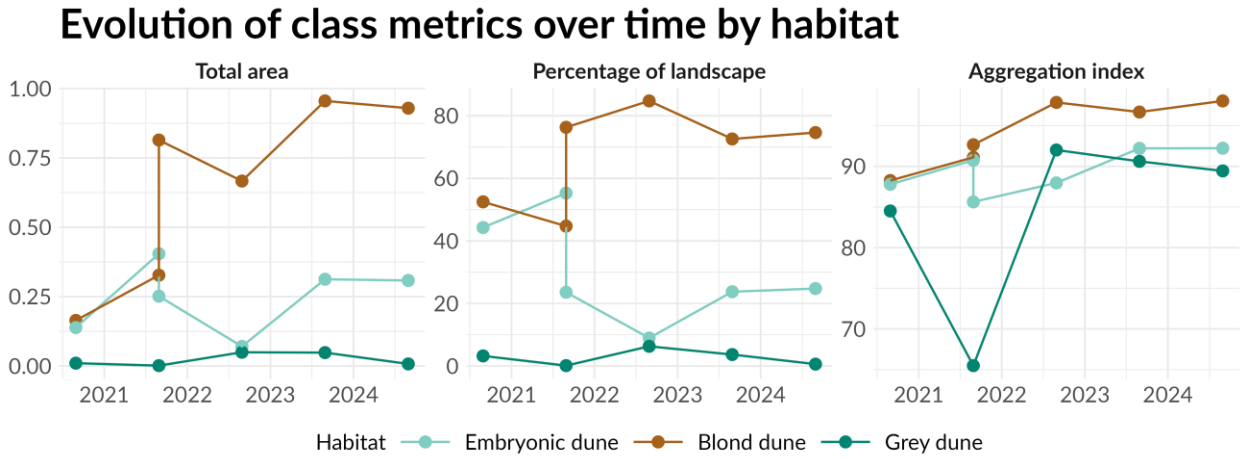

Figure 4.18: RandomForest habitat classification for Middelkerke.

The observation of aerial images in Figure 4.18 highlights that the presence of buildings near the area creates difficulties for monitoring this site with the model, due to strong shadows affecting its ability to identify habitats. However, from 2020 to 2024, the coastal dune habitats—blond dune, embryonic dune, and grey dune—showed distinct temporal trends in area and spatial structure. Blond dunes expanded, increasing from 52.5 to 74.6 percent of the landscape, with their connectivity improving steadily, as shown by a rise in aggregation index to 98.0 by 2024. Embryonic dunes decreased sharply in area until 2022, then partially recovered, while maintaining relatively stable spatial cohesion. Grey dunes remained limited in extent. Two closely spaced data points in 2021, showing distinct values for embryonic and blond dunes, highlight the effect of shadow on the studied area and the importance of image quality for the model.

4.7 Raversijde (Belgium)

4.7.1 Area overview

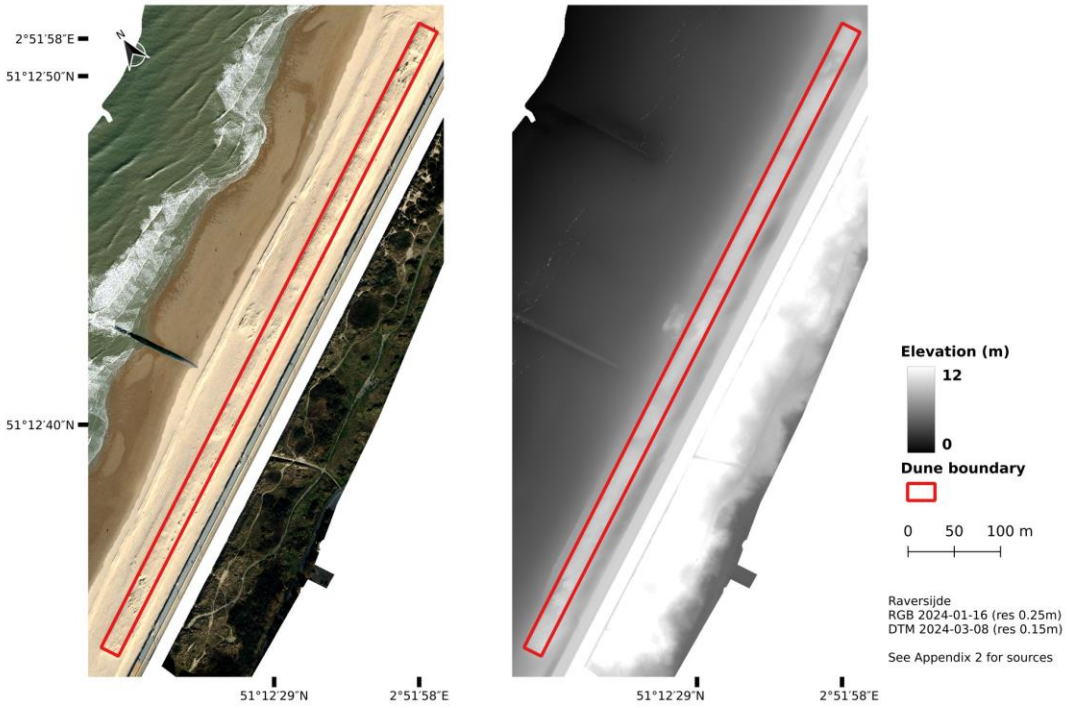

Figure 4.19: Most recent available RGB map (left) and Elevation map (right) for Raversijde.

4.7.2 Habitat cartography

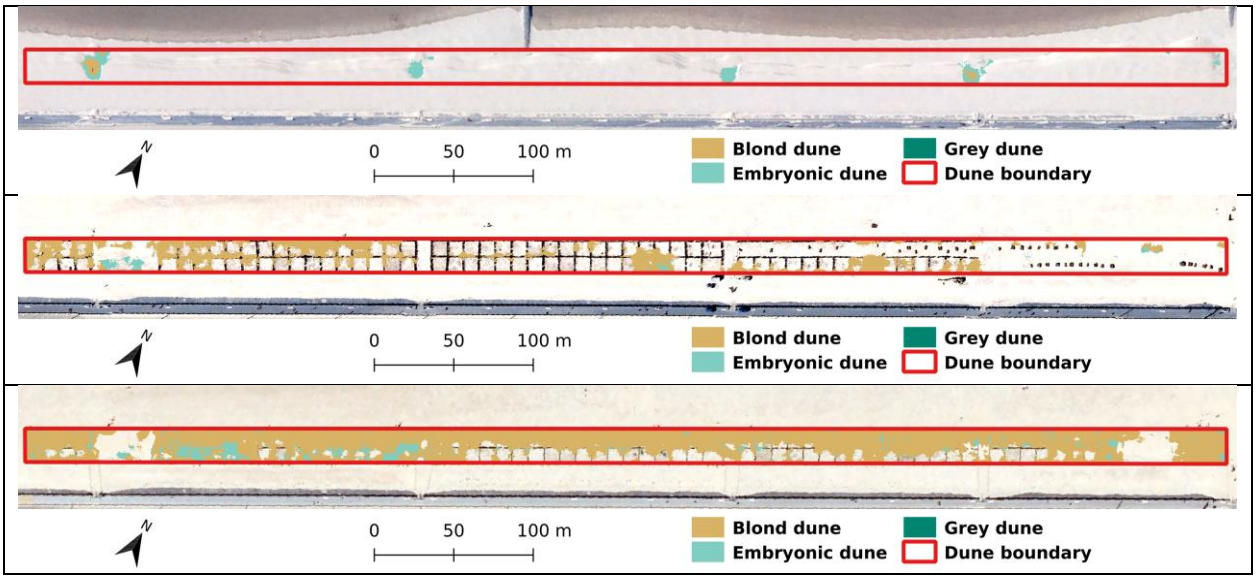

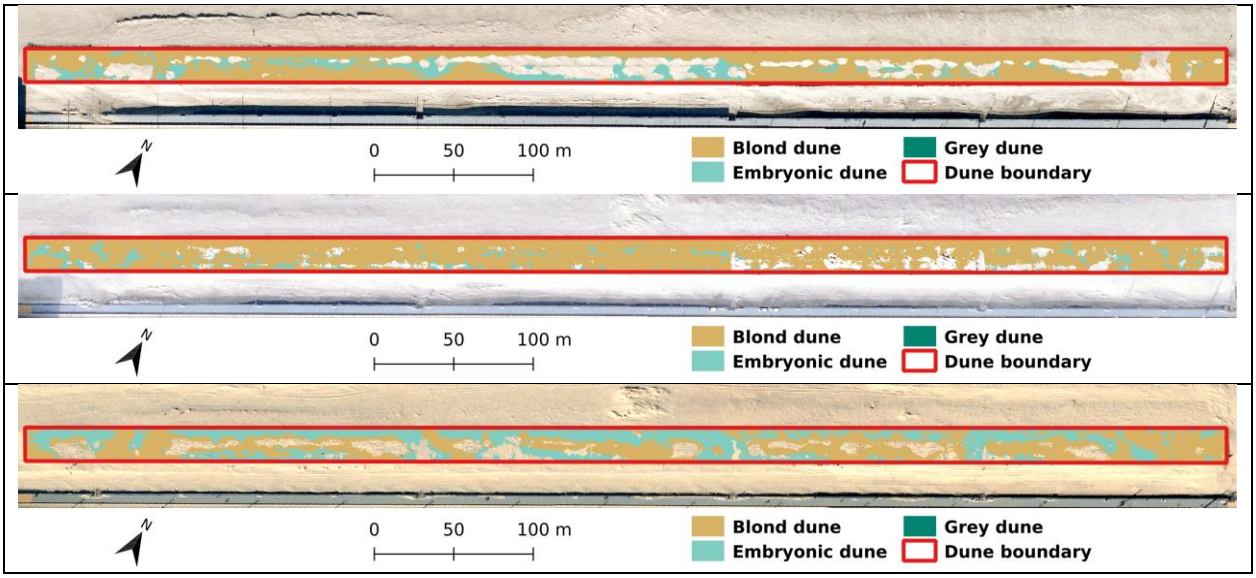

Figure 4.20: RandomForest habitat classification at T1 = 2020-03, T2 = 2021-03, T3 = 2021-07, T4 = 2022-02, T5 = 2023-07, T6 = 2024-03-08 for Raversijde. Classification is overlaid on the corresponding temporal RGB map.

4.7.3 Temporal analysis

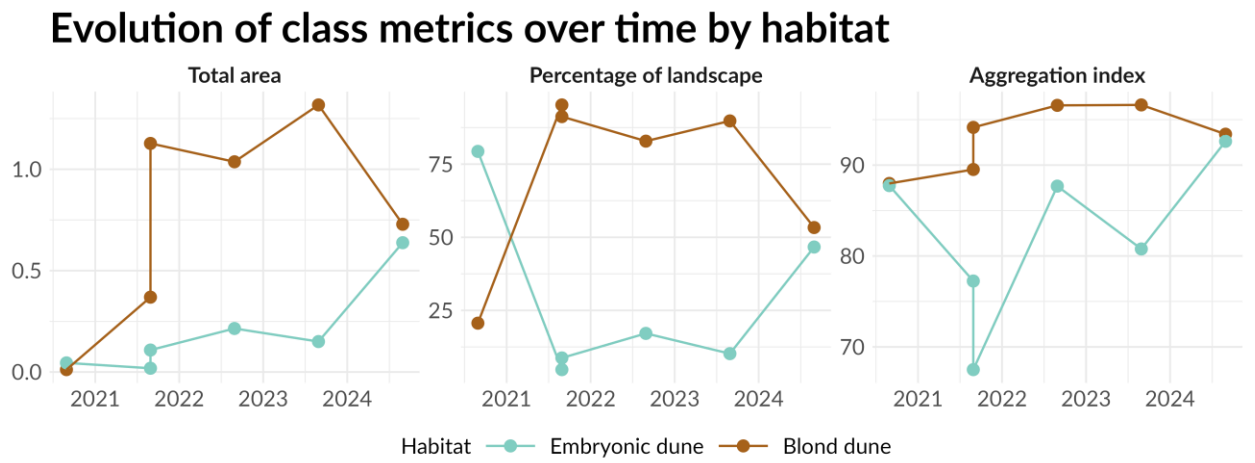

Figure 4.21: RandomForest habitat classification for Raversijde.

Between 2020 and 2023, blond dunes showed a steady increase in both total area and aggregation, indicating expansion and spatial consolidation. However, between 2023 and 2024, this trend reversed: the total area of blond dunes decreased notably, and their aggregation index dropped slightly. In contrast, embryonic dunes experienced a sharp increase during the same period, replacing disappearing blond dune. As other Belgium sites for which intra-annual data are available, Raversijde demonstrator site shows a high intra-annual variability in 2021, particularly for blond dune.

4.8 Sankt Peter-Ording (Germany)

4.8.1 Area overview

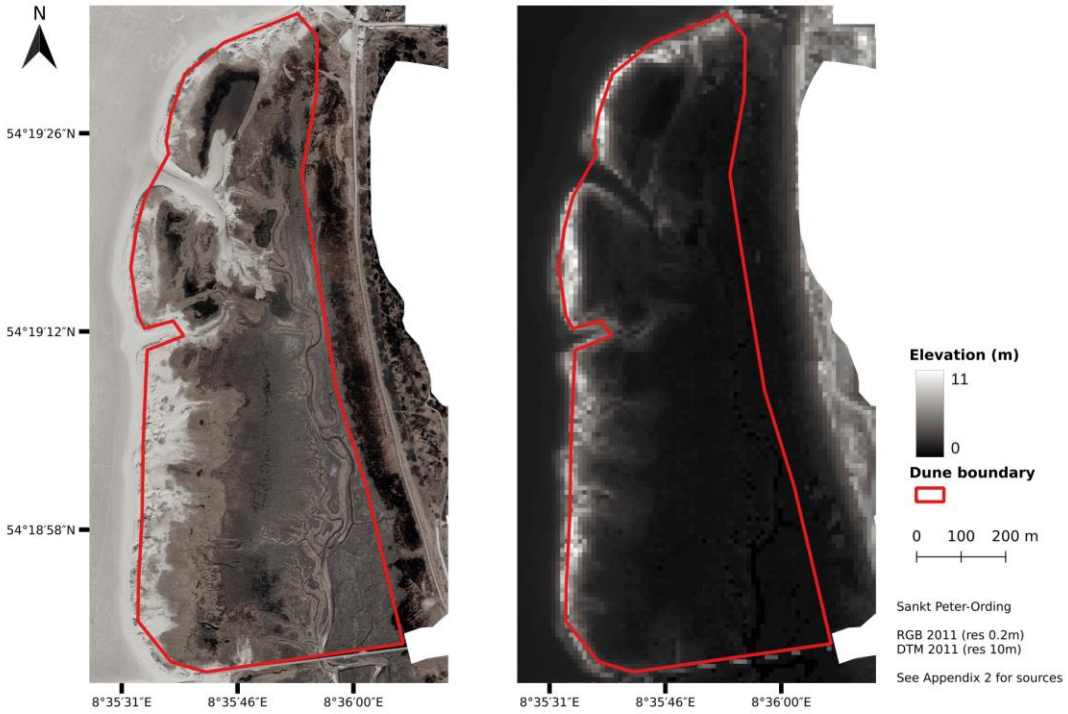

Figure 4.22: Most recent available RGB map (left) and Elevation map (right) for Sankt Peter-Ording.

4.8.2 Habitat cartography

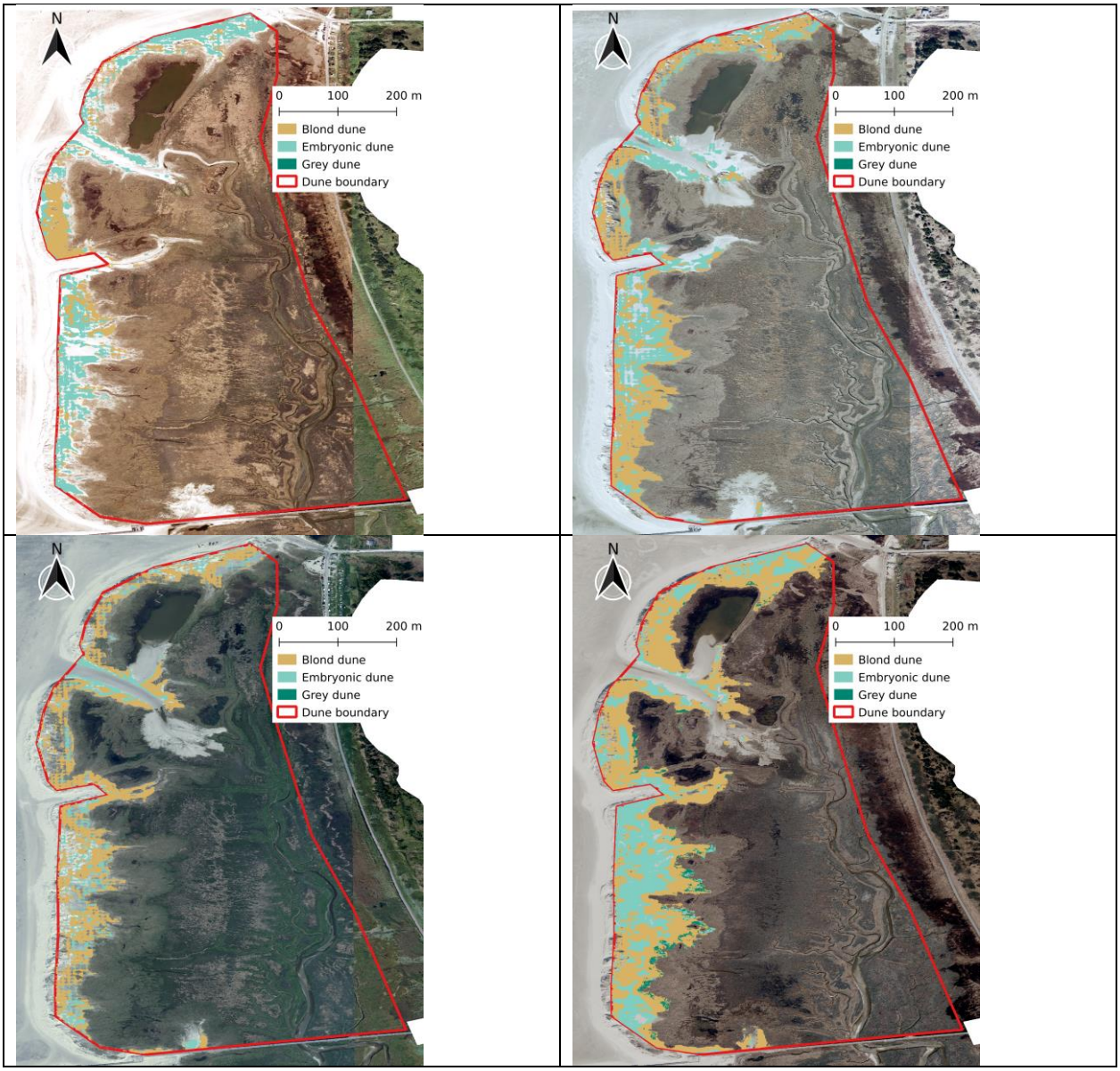

Figure 4.23: RandomForest habitat classification at T1 = 2011, T2 = 2014, T3 = 2017, T4 = 2020 for Sankt Peter-Ording (left to right then top to bottom). Classification is overlaid on the corresponding temporal RGB map.

4.8.3 Temporal analysis

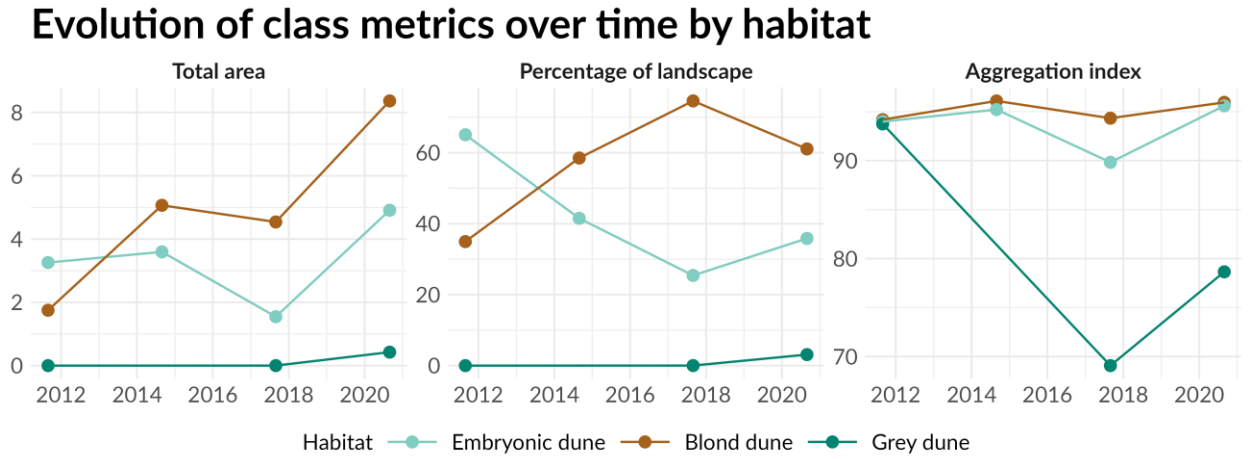

Figure 4.24: Evolution of some landscape metrics in time by habitat for Sankt Peter-Ording

The site exhibits significant dune dynamics between 2011 and 2020. Initially, embryonic dunes dominated the landscape, covering over 65% of the area in 2011, while blond dunes occupied just 35%. Over time, this pattern reversed: by 2017, blond dunes had expanded to nearly 75%, with embryonic dunes reduced to just over 25%. Total area of blond dune expanded since 2011 reaching more that 8% of the total landscape by 2020. Grey dunes, nearly absent at the beginning, gradually appeared, reaching over 3% of the area by 2020. However, fluctuations in grey dune surface could also reflect classification uncertainty, especially in early years when their presence was minimal. It should be noted, however, that T1 is already a long time after the implementation of the demonstrator and that we do not have data before. We also need to underline than embryonic dune reduction in percentage of landscape could also be caused by the demonstrator boundary as predefined, since part of the young dune on the west is outside of the boundary (visible on Figure 8.1). Unclassified land on the right of each image correspond to wetland and have successfully been not classified as dune by the model.

4.9 Soulac (France)

4.9.1 Area overview

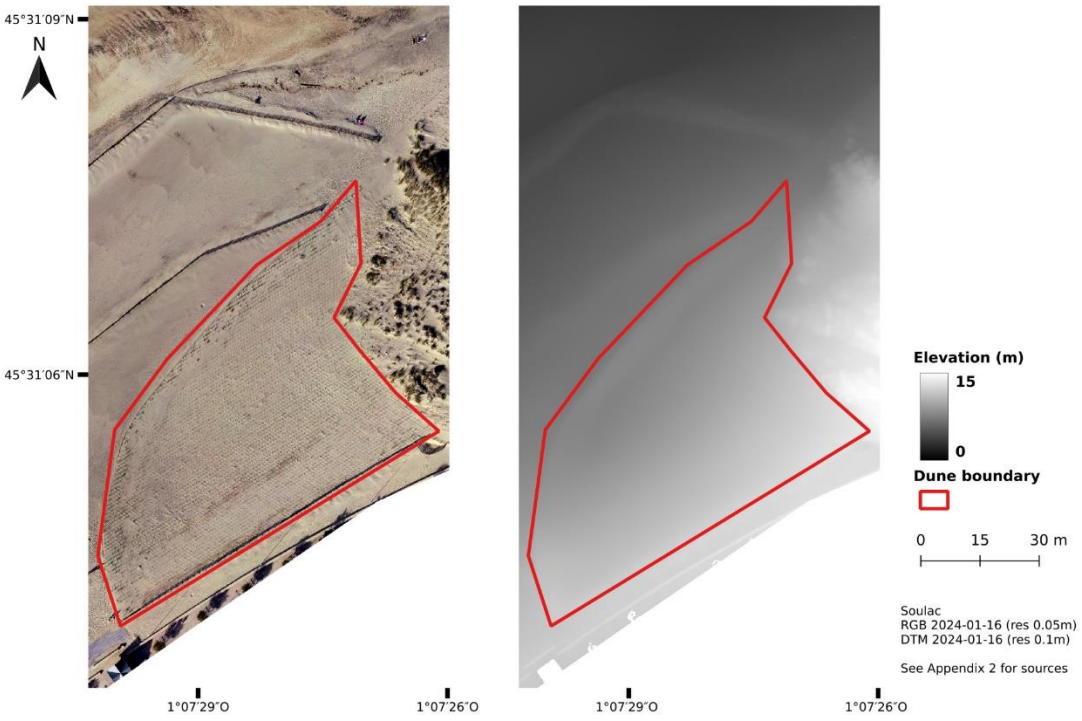

Figure 4.25: Most recent available RGB map (left) and Elevation map (right) for Soulac.

4.9.2 Habitat cartography

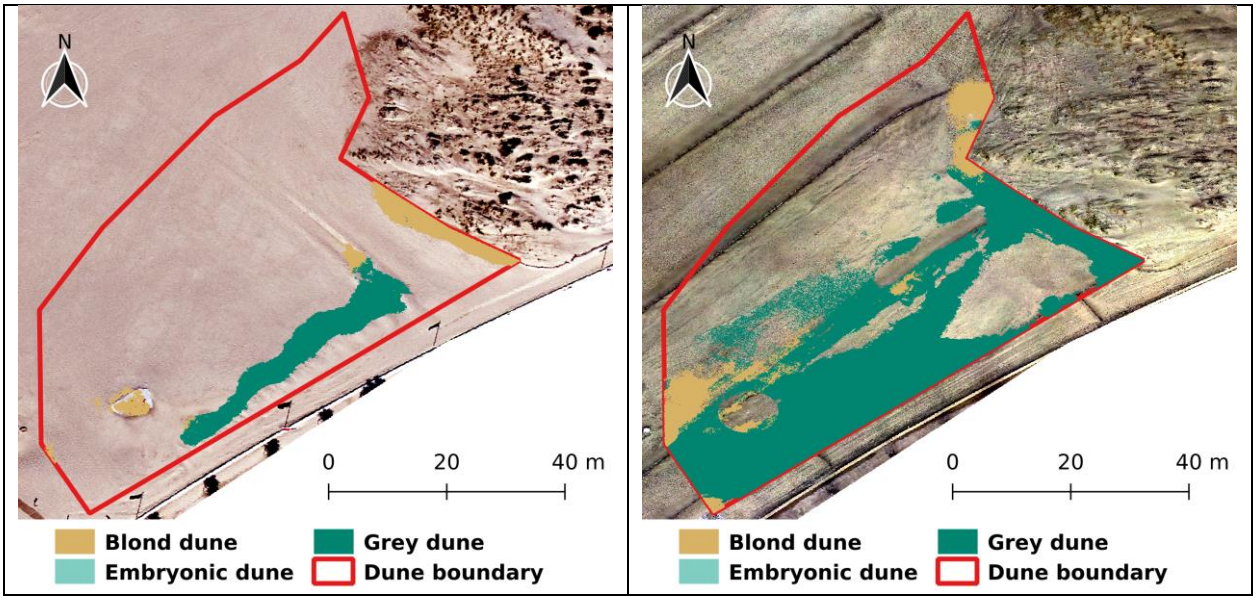

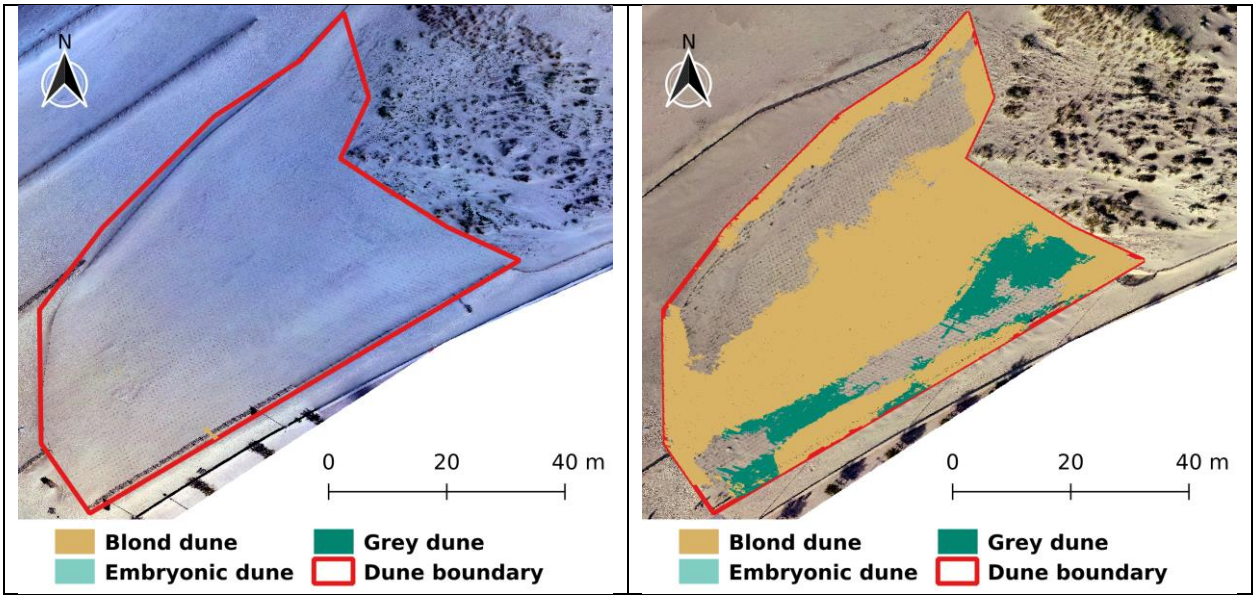

Figure 4.26: RandomForest habitat classification at T1 = 2023-09, T2 = 2024-01, T3 = 2024-04, T4 = 2024-10 for Soulac (left to right then top to bottom). Classification is overlaid on the corresponding temporal RGB map.

4.9.3 Temporal analysis

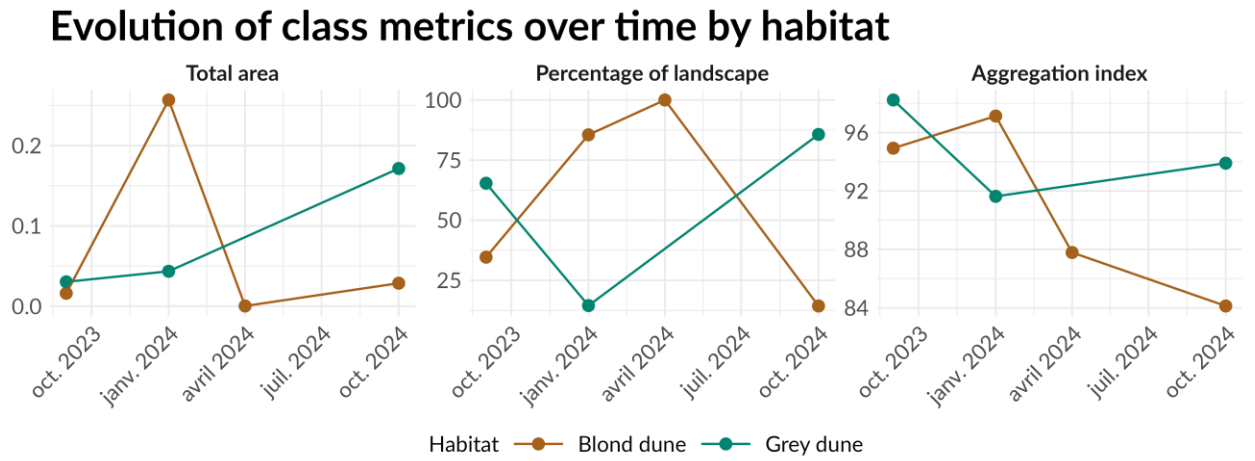

Figure 4.27: Evolution of some landscape metrics in time by habitat for Soulac

The classification of this site—recently planted, relatively flat—poses a challenge for the model. Prior to the plantation in early 2024, an area was classified as grey dune, most likely consisting of embryonic dune patches. Following the plantation, vegetation classification disappeared in the April 2024 observation, while areas classified as grey dune and blond dune emerged in late 2024. The classification of this very young demonstrator site (with the most recent images taken just seven months after plantation) remains a challenge for the model.

Although the Natura 2000 definition of the blond dune habitat is based on the dominance of marram grass—and this species was indeed planted to establish the demonstrator—it may still be too early to confidently classify this area as blond dune.

4.10 Texel (The Netherlands)

4.10.1 Area overview

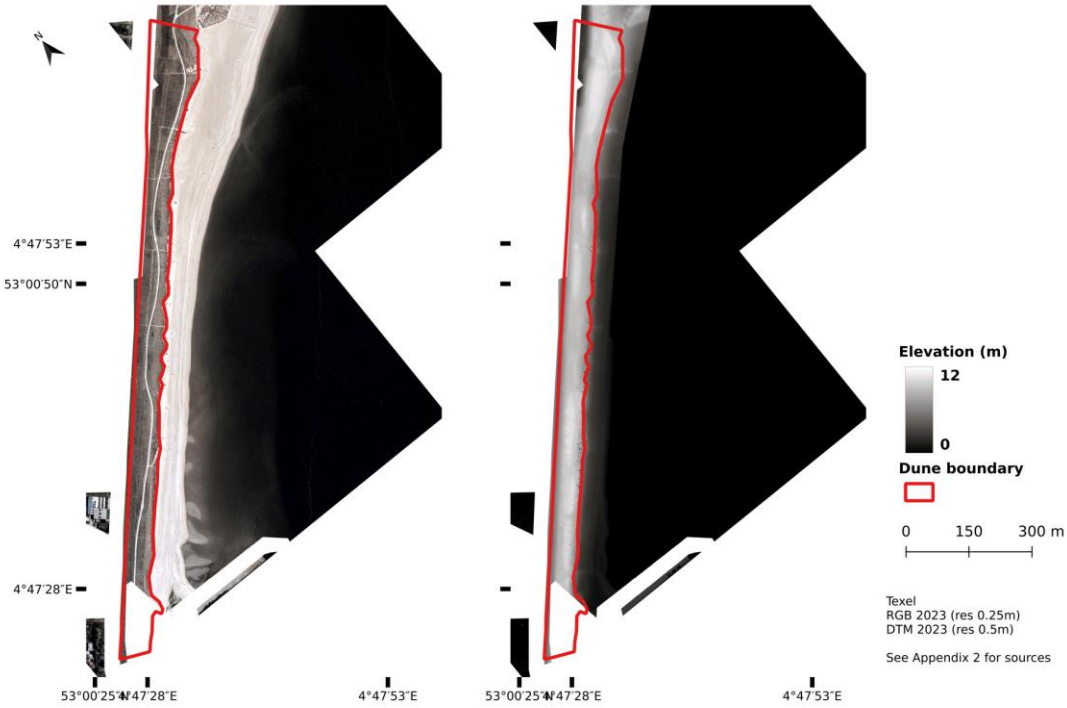

Figure 4.28: Most recent available RGB map (left) and Elevation map (right) for Texel.

4.10.2 Habitat cartography

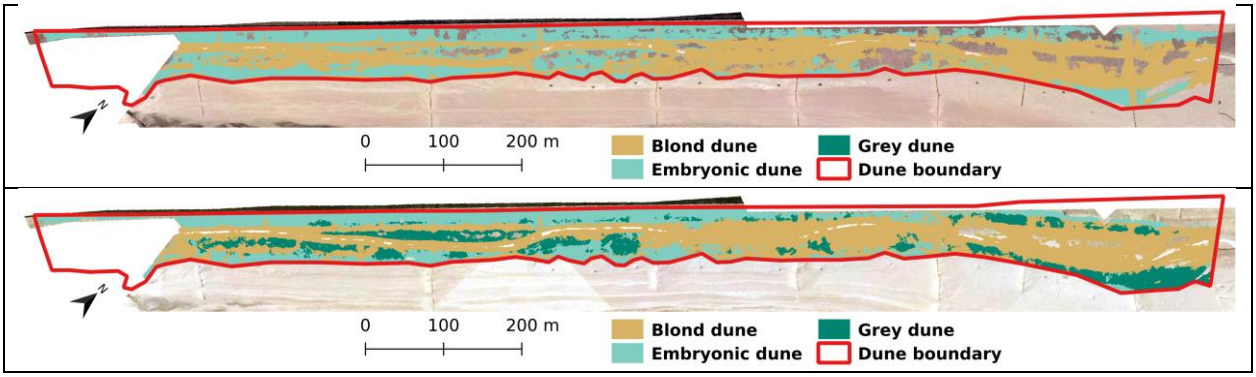

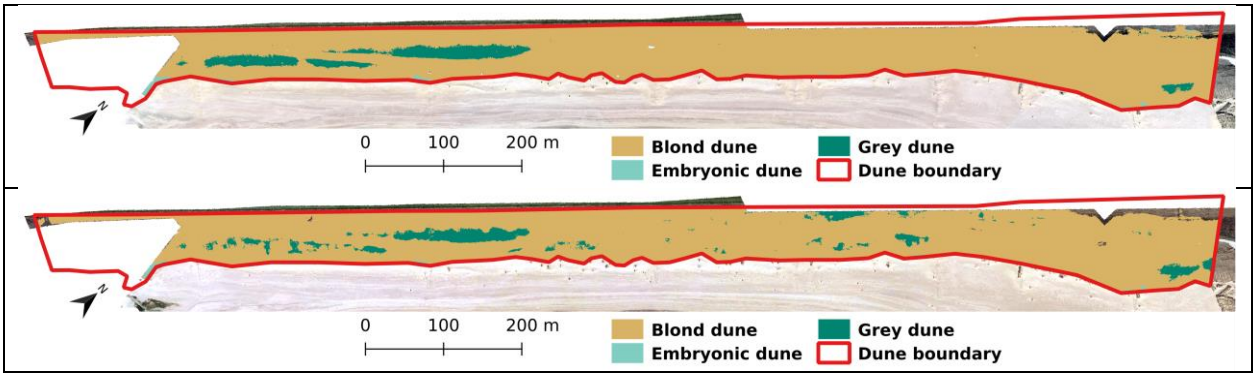

Figure 4.29: RandomForest habitat classification at T1 =2019, T2 = 2020, T3 = 2022, T4 = 2023 for Texel. Classification is overlaid on the corresponding temporal RGB map.

4.10.3 Temporal analysis

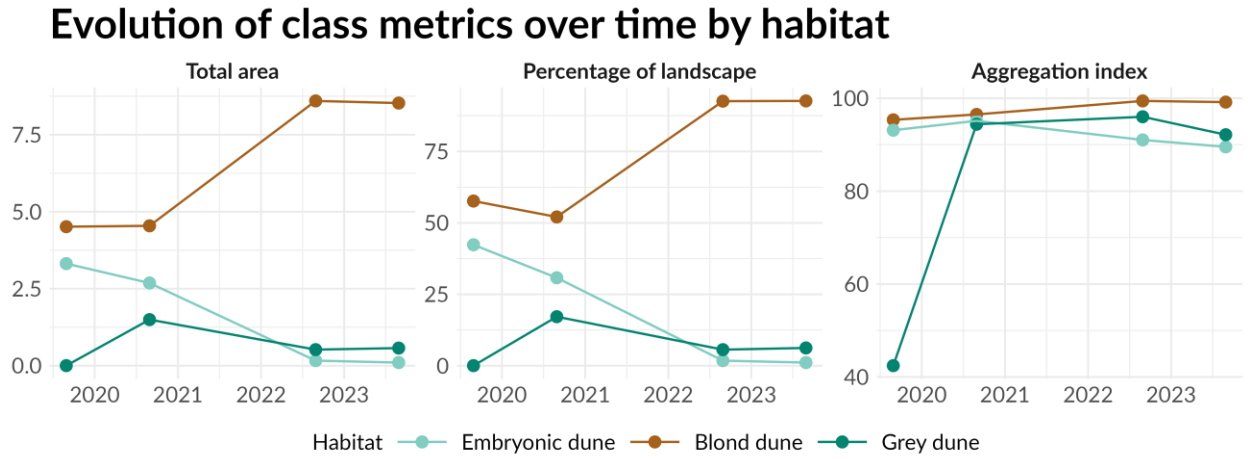

Figure 4.30: Evolution of some landscape metrics in time by habitat for Texel

This site, first monitored in 2019 shortly after the demonstrator was installed, showed a high initial presence of embryonic dunes (42%), which rapidly declined to under 2% by 2022. This sharp decrease reflects limited sediment input and low geomorphological activity. Blond dunes quickly became dominant, rising from 58% to over 92% by 2022 and maintaining very high connectivity (AI >99%), indicating a stable and mature dune system. Grey dunes appeared from the start but always in the same location. Their early presence likely reflects misclassification.

4.11 Ystad (Sweden)

4.11.1 Area overview

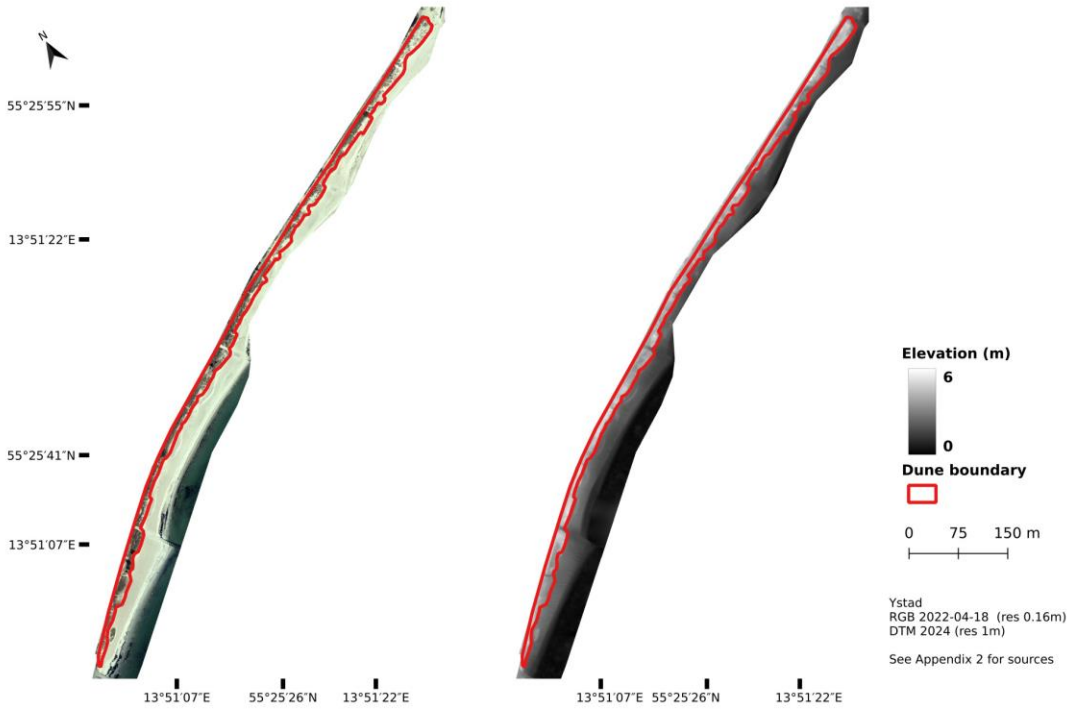

Figure 4.31: Most recent available RGB map (left) and Elevation map (right) for Ystad.

4.11.2 Habitat cartography

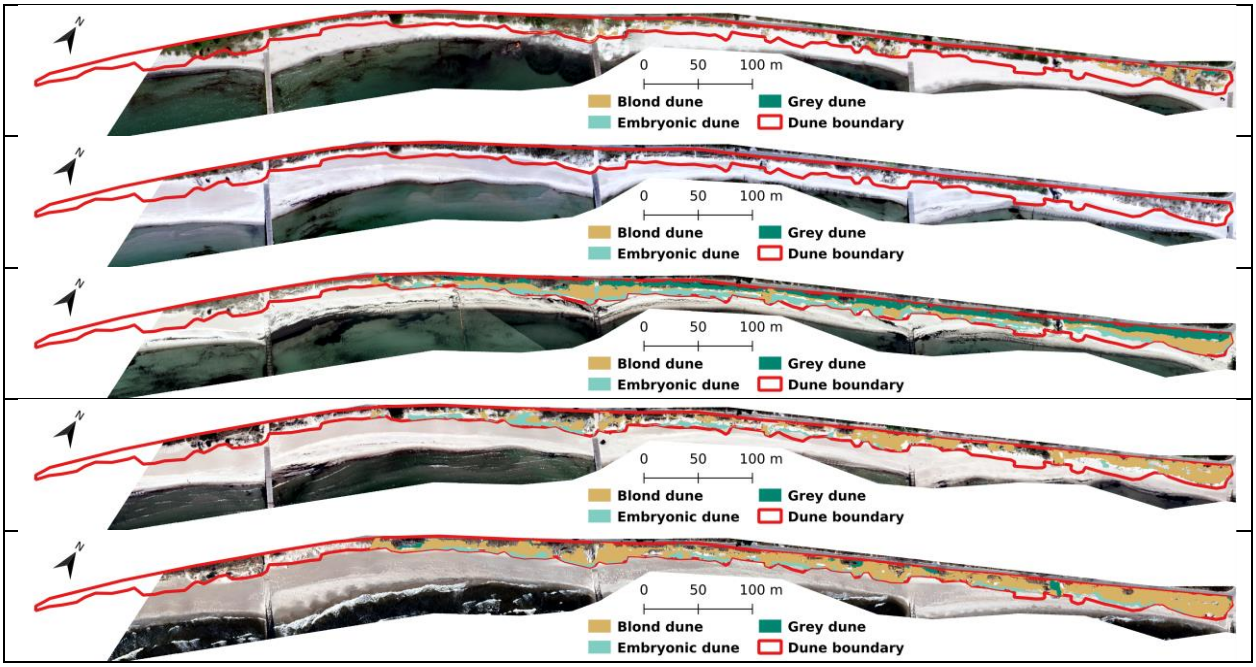

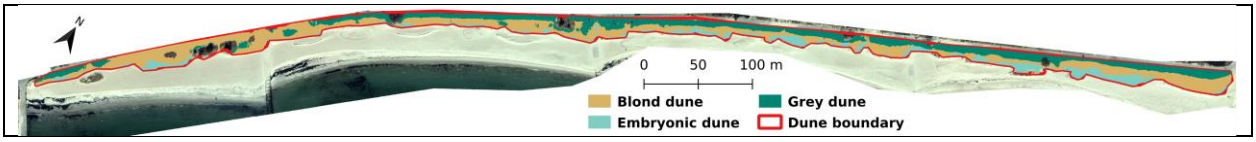

Figure 4.32: RandomForest habitat classification at T1 = 2010-06-04, T2 = 2012-05-02, T3 = 2014-03-31, T4 = 2016-05-13, T5 = 2018-04-11, T6 = 2022-04-18 for Ystad. Classification is overlaid on the corresponding temporal RGB map.

4.11.3 Temporal analysis

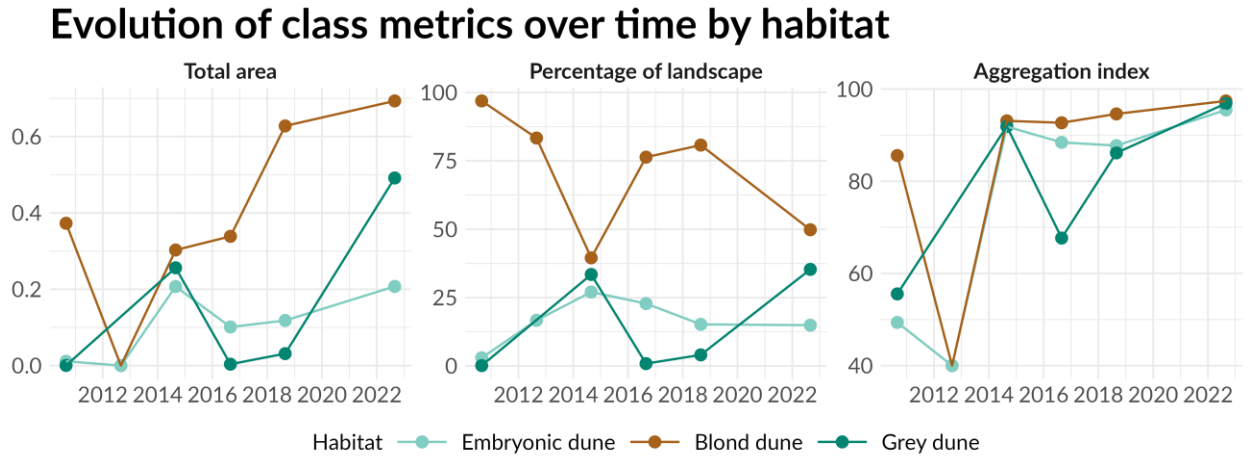

Figure 4.33: Evolution of some landscape metrics in time by habitat for Ystad.

The site, established in 2011, already showed signs of dune vegetation prior to installation, with significant blond dune coverage as early as 2010. Unfortunately, there are no elevation images dating from before 2019 for this site, which may affect the model's prediction quality. Since then, the blond dune has steadily expanded, reaching over 90% of the area by 2023, while embryonic dunes have progressively declined Embryonic dunes were present throughout but remained minor, peaking early and then stabilizing around 15–20% of the area. Grey dunes were more variable, with inconsistent patterns of expansion and regression. The observed variability can likely be attributed to classification challenges: the site's dune is narrow, with limited elevation contrast and close to the waterline, making accurate mapping more difficult for the model.

5. General discussion

The aim of this report was to evaluate the evolution of key dune habitats—defined in Annex I of the EU Habitats Directive—for each demonstrator site (Directorate-General for Environment, European Commission, 2013; Bensettiti et al., 2004). Spectral and topographic data

were collected, and a Random Forest model was used to map the habitats. Temporal changes at each demonstrator were assessed using landscape metrics (**Table 5.1.1**). The model developed to map habitat may also be reused to support analyses in WP5.2 and WP5.3.

Large systems (e.g., Delflandse Kust, Dunkerque, or Sankt Peter-Ording) appear to show dynamic evolution, particularly for the target habitats—embryonic dunes and blond dunes. In contrast, Katwijk and Texel seem to be undergoing succession towards stabilization or even degradation, with an increase in blond dunes and little to no embryonic dune presence. Both habitats are sheltered from the dominant wind—at Katwijk due to temporary summer habitation, and at Texel because of its orientation. These are less dynamic systems, possibly indicating lower resilience. Hondsbossche, despite being a very large system, appears to follow the same trend as the previous two sites. Raversijde and Fort Napoleon, highly dynamic sites that experienced strong sand burial following plantation, now show colonization by embryonic dunes, suggesting that the system is still in the process of establishing. The youngest demonstrator, at Soulac, remains too recent to allow conclusions on the effectiveness of the system.

Table 5.1.1 - Summary of the predictions about habitat evolution for the demonstrators in this deliverable

Name	Grey dune	Blond dune	Embryonic dune
Delflandse kust	Increase	Increase	Increase
Dunkerque	No	Stable	Increase
Fort Napoleon	No	Decrease	Increase
Hondsbossche	Stable to increase	Increase	Stable to decrease
Katwijk	Stable to increase	Stable to increase	Decrease
Middelkerke	Stable to decrease	Increase	Stable to increase
Raversijde	No	Decrease	Increase
Sankt Peter Ording	No	Increase	Increase
Soulac	No	Stable to increase	No
Texel	?	Increase	Decrease
Ystad	Increase	Increase	Increase

Some limitations may also arise from differences between training and validation datasets. While validation was based on manually drawn, object-based shapes, the model operates at the pixel level. This scale mismatch can lead to misclassifications, especially due to the limited precision of the manually drawn polygons. Moreover, the model was trained and tested on selected images that clearly depict habitat features, which can reduce accuracy when applied to lower-quality images or more complex habitat structures. Continuing on the pixel

level at which the model operates and its consequences, a post-processing step aggregating predicted pixels into consistent patches/clusters of a minimal meaningful size, using hole-filling algorithms as needed, may reduce noise in predictions (Eurostat (European Commission), 2021).

Data collection conditions also pose challenges. Vegetation phenology affects both plant color, and presence for annual species. Images taken in winter may fail to capture embryonic vegetation or misidentify dead plants that will regrow in the following season. Using extended phenotypic data, incorporating spatial variability and elevation indices rather than relying solely on spectral indices, can partially address these issues.

This deliverable represents an intermediate step in the development of coastal dune habitat mapping methods. The overarching objective is to develop and publish a scientific article on innovative approaches for mapping Natura 2000 coastal dune habitats. The ability to accurately map habitats such as grey dunes and embryonic dunes may be improved through additional steps that are currently under consideration and planning.

The next planned steps include more spatial autocorrelation measures, such as Moran's I (Moran, 1950), and adding variation coefficients for neighborhood and transect indices. Other classification methods will also be explored, including semi-supervised approaches like Self-Organizing Maps (SOM), and combinations such as Singular Value Decomposition (SVD)—a technique similar to Principal Component Analysis (PCA)—with k-means clustering. These methods aim to group pixels into habitat categories corresponding to Natura 2000 types. Their effectiveness will be evaluated, with particular attention to the mapping accuracy of embryonic dunes (2110) and drift lines (1210).

The semi-supervised approach does not rely on predefined training datasets but instead uses known reference areas with ground-truth habitat information to guide the selection of algorithm parameters. This method aims to develop a model that can be generalized beyond the specific study area, offering better control over the variable characteristics of each habitat. It also allows for the observation of broader pixel-level variation, potentially moving beyond strict habitat classifications toward a gradient-based interpretation. This approach is expected to identify threshold values or index definitions for each variable of interest that correspond to specific Natura 2000 habitats. These thresholds could be reused by municipalities or coastal managers to map Natura 2000 coastal habitats across Europe. Nevertheless, the use of the Random Forest model in this deliverable already yields promising results in coastal habitat mapping—particularly for embryonic dunes, with a final sensitivity of 77% despite their scattered and sparse nature.

6. References

Agrillo, E., Filipponi, F., Salvati, R., Pezzarossa, A., & Casella, L. (2023). Modeling approach for coastal dune habitat detection on coastal ecosystems combining very high-resolution UAV imagery and field survey. *Remote Sensing In Ecology And Conservation*, 9(2), 251-267. https://doi.org/10.1002/rse2.308

Barnes, R., Lehman, C., & Mulla, D. (2013). Priority-flood : An optimal depression-filling and watershed-labeling algorithm for digital elevation models. *Computers & Geosciences*, 62, 117-127. https://doi.org/10.1016/j.cageo.2013.04.024

Bell, W. D., Visser, V., Kirsten, T., & Hoffman, M. T. (2022). An evaluation of different approaches which use Google Street View imagery to ground truth land degradation assessments. *Environmental Monitoring And Assessment*, 194(10). https://doi.org/10.1007/s10661-022-10438-5

Bensettiti F., Bioret F., Roland J. & Lacoste J.-P. (coord.), 2004. *« Cahiers d'habitats » Natura 2000. Connaissance et gestion des habitats et des espèces d'intérêt communautaire. Tome 2 - Habitats côtiers*. MEDD/MAAPAR/MNHN. Éd. La Documentation française, Paris, 399 p.

Castelle, B., Dahirel, M. (2024). *Physical boundary conditions, Version 1.0*, DuneFront Project Deliverable 4.1, Université de Bordeaux

Croft, H., Chen, J. M., & Zhang, Y. (2014). The applicability of empirical vegetation indices for determining leaf chlorophyll content over different leaf and canopy structures. *Ecological Complexity*, 17, 119-130. https://doi.org/10.1016/j.ecocom.2013.11.005

Directorate-General for Environment, European Commission. (2013). *Interpretation manual of European Union habitats – EUR28*. https://eunis.eea.europa.eu/references/2435

Dormann, C. F., Elith J., Bacher S., Buchmann C., Carl G., Carré G., Marquéz J.R.G., Gruber B., Lafourcade B., Leitão P.J., Münkemüller T., McClean C., Osborne P., Reineking B., Schröder B., Skidmore A., Zurell D., & Lautenbach S. (2013). Collinearity: a review of methods to deal with it and a simulation study evaluating their performance. *Ecography* 37, 27-46. https://doi.org/10.1111/j.1600-0587.2012.07348.x

Eurostat (European Commission). (2021). *Applying the degree of urbanisation: A methodological manual to define cities, towns and rural areas for international comparisons : 2021 edition*. Publications Office of the European Union. https://doi.org/10.2785/706535

Hesselbarth, M. H. K., Sciaini, M., With, K. A., Wiegand, K., & Nowosad, J. (2019). landscapemetrics : an open-source R tool to calculate landscape metrics. *Ecography*, 42(10), 1648-1657. https://doi.org/10.1111/ecog.04617

Laporte-Fauret, Q., Lubac, B., Castelle, B., Michalet, R., Marieu, V., Bombrun, L., Launeau, P., Giraud, M., Normandin, C., & Rosebery, D. (2020). Classification of Atlantic Coastal Sand Dune Vegetation Using In Situ, UAV, and Airborne Hyperspectral Data. *Remote Sensing*, 12(14), 2222. https://doi.org/10.3390/rs12142222

Lu, N., Zhou, J., Han, Z. et al. (2019). Improved estimation of aboveground biomass in wheat from RGB imagery and point cloud data acquired with a low-cost unmanned aerial vehicle system. *Plant Methods*, 15, 17. https://doi.org/10.1186/s13007-019-0402-3

Marcenò, C., Guarino, R., Loidi, J., Herrera, M., Isermann, M., Knollová, I., Tichý, L., Tzonev, R. T., Acosta, A. T. R., FitzPatrick, Ú., Iakushenko, D., Janssen, J. A. M., Jiménez-Alfaro, B., Kącki, Z., Keizer-Sedláková, I., Kolomiychuk, V., Rodwell, J. S., Schaminée, J. H. J., Šilc, U., & Chytrý, M. (2018). Classification of European and Mediterranean coastal dune vegetation. *Applied Vegetation Science*, 21(3), 533-559. https://doi.org/10.1111/avsc.12379

Marzialetti, F., Giulio, S., Malavasi, M., Sperandii, M. G., Acosta, A. T. R., & Carranza, M. L. (2019). Capturing Coastal Dune Natural Vegetation Types Using a Phenology-Based Mapping Approach: The Potential of Sentinel-2. *Remote Sensing*, 11(12), 1506.

Maun, M. A. (2009). The Biology of Coastal Sand Dunes. Oxford University Press.

Moran, P. A. P. (1950). Notes on continuous stochastic phenomena. *Biometrika*, 37(1-2), 17–23, https://doi.org/10.1093/biomet/37.1-2.17

QGIS Development Team, 2022. *QGIS Geographic Information System*. Open Source Geospatial Foundation. URL http://qgis.org

R Core Team (2021). *R: A language and environment for statistical computing*. R Foundation for Statistical Computing, Vienna, Austria. URL https://www.R-project.org/.

Robin, N., Ruz, M-H., Castelle, B., Blaise, E., 2025. *Morphodynamics patterns, DuneFront Project Deliverable 6.1*.

van Puijenbroek, M. E. B., Nolet, C., de Groot, A. V., Suomalainen, J. M., Riksen, M. J. P. M., Berendse, F., & Limpens, J. (2017). Exploring the contributions of vegetation and dune size to early dune development using unmanned aerial vehicle (UAV) imaging. *Biogeosciences*, 14, 5533–5549. https://doi.org/10.5194/bg-14-5533-2017

Wright, M. N., & Ziegler, A. (2017). ranger : A Fast Implementation of Random Forests for High Dimensional Data in C++ and R. *Journal Of Statistical Software*, 77(1). https://doi.org/10.18637/jss.v077.i01

Yuke, Zhou. (2019). Greenness Index from Phenocams Performs Well in Linking Climatic Factors and Monitoring Grass Phenology in a Temperate Prairie Ecosystem. *Journal of Resources and Ecology*. 10. 481. https://doi.org/10.5814/j.issn.1674-764x.2019.05.003

Zvoleff, A., (2014). *glcm: Calculate Textures from Grey-Level Co-Occurrence Matrices (GLCMs)*. R package version 1.6.5, https://cran.r-project.org/web/packages/glcm. Accessed 16 Jul. 2025.

7. Appendices

7.1 Table A1 - Variables selected and used in the model

CATEGORY	VARIABLE NAME	DESCRIPTION
COLORSPACE INDEX	Hue	Position of a pixel RGB color on a chromatic circle
	Saturation	Pixel color intensity (vivid or muted)
	A	Color axis between green (negative values) and red (positive values)
	B	Color axis between blue (negative values) and yellow (positive values)
STANDARD INDEX	Green	Green intensity in a pixel
	Elevation (m)	Elevation at a pixel
	BGI	Blue Green pigment index
	GCC	Green Chromatic Coordinate index
	NPCI	Normalized Pigment Chlorophyll index
TEXTURE INDEX	glcm_G_contrast	Measures texture contrast in the green band around each pixel
	glcm_G_entropy	Measures randomness in green band textures around each pixel
	glcm_G_second_moment	Measures texture uniformity in green values around each pixel
	glcm_E_mean	Measures average elevation texture intensity around each pixel
	glcm_E_homogeneity	Measures smoothness in elevation textures around each pixel
	glcm_E_contrast	Measures elevation texture variation around each pixel
	glcm_E_dissimilarity	Measures elevation texture difference around each pixel
	glcm_E_entropy	Measures randomness in elevation textures around each pixel
	Aspect	Calculates aspect as the direction of the maximum slope of the focal cell
	Planform curvature	Calculated by fitting a surface to the focal cell and its neighbours. The planform curvature runs perpendicular to the maximum slope of this surface and affects the convergence and divergence of flow down the slope
	Profiles curvature	Calculated by fitting a surface to the focal cell and its neighbours. The profile curvature runs parallel to the maximum slope of this surface and affects the acceleration and deceleration of flow down the slope.
NEIGHBORHOOD INDEX	mean_Green	Mean of the green band within a 5-meter radius
	mean_Elevation	Mean of the elevation band within a 5-meter radius
	mean_BGI	Mean of the Blue Green pigment index within a 5-meter radius

	mean_GCC	Mean of the Green Chromatic Coordinate index within a 5-meter radius
	mean_ExB	Mean of the Excess Blue index within a 5-meter radius
	mean_mGRVI	Mean of the modified Green Red Vegetation Index within a 5-meter radius
	max_Elevation	Maximum value of the elevation band within a 5-meter radius
	max_BGI	Maximum value of the Blue Green pigment index within a 5-meter radius
	max_NPCI	Maximum of the Normalized Pigment Chlorophyll index within a 5-meter radius
	max_ExB	Maximum of the Excess Blue index within a 5-meter radius
	min_Green	Minimum of the green band within a 5-meter radius
	min_Elevation	Minimum of the elevation band within a 5-meter radius
	min_BGI	Minimum of the Blue Green pigment index within a 5-meter radius
	min_GCC	Minimum of the Green Chromatic Coordinate index within a 5-meter radius
	min_NPCI	Minimum of the Normalized Pigment Chlorophyll index within a 5-meter radius
	min_ExB	Minimum of the Excess Blue index within a 5-meter radius
	min_mGRVI	Minimum of the modified Green Red Vegetation Index within a 5-meter radius
	stddev_Green	Standard deviation of the green band within a 5-meter radius
	stddev_Elevation	Standard deviation of the elevation band within a 5-meter radius
	stddev_BGI	Standard deviation of the Blue Green pigment index within a 5-meter radius
	stddev_GCC	Standard deviation of the Green Chromatic Coordinate index within a 5-meter radius
	stddev_NPCI	Standard deviation of the Normalized Pigment Chlorophyll index within a 5-meter radius
	stddev_ExB	Standard deviation of the Excess Blue index within a 5-meter radius
	stddev_mGRVI	Standard deviation of the modified Green Red Vegetation Index within a 5-meter radius
	percentile95_Elevation	95th percentile of the elevation band within a 5-meter radius
	percentile95_NPCI	95th percentile of the Normalized Pigment Chlorophyll index within a 5-meter radius
	percentile95_ExB	95th percentile of the Excess Blue index within a 5-meter radius
TRANSECT INDEX	meanV_Elevation	Mean of the elevation band within a cross-shore transect of 5-meter range
	maxV_Elevation	Maximum of the elevation band within a cross-shore transect of 5-meter range
	minV_Elevation	Minimum of the elevation band within a cross-shore transect of 5-meter range

minV_BGI	Minimum of the Blue Green pigment index within a cross-shore transect of 5-meter range
minV_ExB	Minimum of the Excess Blue index within a cross-shore transect of 5-meter range
stddevV_Green	Standard deviation of the green band within a cross-shore transect of 5-meter range
stddevV_Elevation	Standard deviation of the elevation band within a cross-shore transect of 5-meter range
stddevV_BGI	Standard deviation of the Blue Green pigment index within a cross-shore transect of 5-meter range
stddevV_GCC	Standard deviation of the Green Chromatic Coordinate index within a cross-shore transect of 5-meter range
stddevV_NPCI	Standard deviation of the Normalized Pigment Chlorophyll index within a cross-shore transect of 5-meter range
stddevV_ExB	Standard deviation of the Excess Blue index within a cross-shore transect of 5-meter range
stddevV_ExG	Standard deviation of the Excess Green index within a cross-shore transect of 5-meter range
stddevV_mGRVI	Standard deviation of the modified Green Red Vegetation Index within a cross-shore transect of 5-meter range
percentile95V_Elevation	95th percentile of the elevation band within a cross-shore transect of 5-meter range
meanH_Green	Mean of the green band within a long-shore transect of 5-meter range
meanH_Elevation	Mean of the elevation band within a long-shore transect of 5-meter range
meanH_GCC	Mean of the Green Chromatic Coordinate index within a long-shore transect of 5-meter range
meanH_NPCI	Mean of the Normalized Pigment Chlorophyll index within a long-shore transect of 5-meter range
maxH_Elevation	Maximum of the elevation band within a long-shore transect of 5-meter range
maxH_BGI	Maximum of the Blue Green pigment index within a long-shore transect of 5-meter range
maxH_GCC	Maximum of the Green Chromatic Coordinate index within a long-shore transect of 5-meter range
maxH_ExB	Maximum of the Excess Blue index within a long-shore transect of 5-meter range
minH_Elevation	Minimum of the elevation band within a long-shore transect of 5-meter range
minH_BGI	Minimum of the Blue Green pigment index within a long-shore transect of 5-meter range
stddevH_Green	Standard deviation of the green band within a long-shore transect of 5-meter range
stddevH_Elevation	Standard deviation of the elevation band within a long-shore transect of 5-meter range
stddevH_BGI	Standard deviation of the Blue Green pigment index within a long-shore transect of 5-meter range

	stddevH_GCC	Standard deviation of the Green Chromatic Coordinate index within a long-shore transect of 5-meter range
	stddevH_NPCI	Standard deviation of the Normalized Pigment Chlorophyll index within a long-shore transect of 5-meter range
	stddevH_ExB	Standard deviation of the Excess Blue index within a long-shore transect of 5-meter range
	stddevH_mGRVI	Standard deviation of the modified Green Red Vegetation Index within a long-shore transect of 5-meter range
	percentile95H_Green	95th percentile of the green band within a long-shore transect of 5-meter range
	percentile95H_Elevation	95th percentile of the elevation band within a long-shore transect of 5-meter range
	percentile95H_BGI	95th percentile of the Blue Green pigment index within a long-shore transect of 5-meter range
	percentile95H_GCC	95th percentile of the Green Chromatic Coordinate index within a long-shore transect of 5-meter range
	percentile95H_NPCI	95th percentile of the Normalized Pigment Chlorophyll index within a long-shore transect of 5-meter range
	percentile95H_ExB	95th percentile of the Excess Blue index within a long-shore transect of 5-meter range
DISTANCE	DISTANCE	Distance between the coastline and the pixel
	DISTANCE_NORM	Distance between the coastline and the pixel normalized by demonstrators

7.2 Table A2 - Available data

Available data for each implemented demonstrator site and minimum temporal gap matching for spectral and elevation images. Data are grouped by demonstrator site or by country when extracted at a national scale. "DFP" refers to data provided by DuneFront partners, while "PAD" indicates publicly available data. For publicly available data, sources are listed below each group name. The left columns present elevation data; the right columns present spectral data. For elevation data: DTM = Digital Terrain Model, DSM = Digital Surface Model, and DEM = Digital Elevation Model. The second column shows the resolution in meters. Simultaneous spectral and elevation surveys either right before or after the implantation date are highlighted in light blue. To reduce the computation time and because images are close by in time, not all Dunkerque (France) available data were used.

Germany								
Sankt Peter-Ording implantation in 1985								
DTM	10	1996	DFP					
DTM	10	1997	DFP					
DTM	10	1998	DFP					
DTM	10	1999	DFP					

DTM	10	2000	DFP					
DTM	10	2001	DFP					
DTM	10	2002	DFP					
DTM	10	2003	DFP					
DTM	10	2004	DFP					
DTM	10	2005	DFP					
DTM	10	2006	DFP					
DTM	10	2007	DFP					
DTM	10	2008	DFP					
DTM	10	2009	DFP					
DTM	10	2010	DFP					
DTM	10	2011	DFP	RGB	0.2	2011	DFP	1
DTM	10	2012	DFP					
DTM	10	2013	DFP					
DTM	10	2014	DFP	RGB	0.2	2014	DFP	2
DTM	10	2015	DFP					
DTM	10	2016	DFP					
DTM	10	2017	DFP	RGB	0.2	2017 / 2018	DFP	3
DTM	10	2019	DFP					
DTM	10	2020	DFP	RGB+NIR	0.2	2020	DFP	4
DTM	10	2021	DFP					
DTM	10	2022	DFP					
Belgium								
Raversijde implantation in 2020 Middelkerke implantation in 2020 Fort Napoleon implantation in 2021								
Sources: https://download.vlaanderen.be/ (Vlaanderen Gouvernement); Digitaal Terrein Model, 25 cm, LiDAR najaarsvlucht strand 2024, Afdeling Kust								
DTM	*1*	*2013-12-10*	*PAD*					
DTM	*1*	*2013-04-29*	*PAD*	*RGB+NIR*	*0.4*	*2012-07*	*PAD*	
DTM	*1*	*2014-04-15*	*PAD*					
DTM	*1*	*2014-11-06*	*PAD*					
DTM	*1*	*2015-05-17*	*PAD*	*RGB+NIR*	*0:4*	*2015-06*	*PAD*	
DTM	*1*	*2015-10-27*	*PAD*					
DTM	*1*	*2016-04-11*	*PAD*	*RGB*	*0.25*	*2016-04*	*PAD*	
DTM	*1*	*2016-12-14*	*PAD*					
DTM	*1*	*2017-05-26*	*PAD*	*RGB*	*0.25*	*2017-03*	*PAD*	
DTM	*1*	*2017-11-06*	*PAD*	*RGB*	*0.25*	*2018-02*	*PAD*	
DTM	*1*	*2018-04-17*	*PAD*	*RGB+NIR*	*0.4*	*2018-07*	*PAD*	
DTM	*1*	*2019-04-20*	*PAD*	*RGB*	*0.25*	*2019-01*	*PAD*	
DTM	1	2018-11-06	PAD	RGB	0.25	2020-03	PAD	1

DTM	1	2019-10-29	PAD					
DTM	1	2020-02-28	PAD					
DTM	1	2020-02-28	PAD					
DTM	1	2020-04-10	PAD					
DTM	1	2020-11-18	PAD					
DTM	0.5	2021-02-16	PAD	RGB	0.25	2021-03	PAD	2
DTM	0.5	2021-02-16	PAD	RGB+NIR	0.4	2021-07	PAD	3
DTM	1	2022-02-23	PAD	RGB	0.15	2022-02	PAD	4
DTM	1	2022-04-17	PAD					
DTM	1	2023-02-08	PAD	RGB	0.15	2023-02	PAD	5
DTM	1	2023-06-17	PAD					
DTM	0.25	2024-01-16	PAD	RGB	0.15	2024-03-08	PAD	6
France								
Dunkerque implantation in 2015 (East site) 2020 (West site)								
DTM	0.5	2008-05-08	DFP					
DTM	1	2011-03-21	DFP					
DTM	1	2014-01-18	DFP					
DTM	0.2	2019-06-03	DFP	RGB	0.2	2018-05-07	DFP	1
DTM	0.2	2020-09-20	DFP	RGB	0.2	2020-09-20	DFP	2
DTM	0.2	2021-04-27	DFP	RGB	0.1	2021-04-27	DFP	3
DTM	1	2020-09-20	DFP	RGB	0.2	2021-06-09	DFP	
DTM	0.2	2021-11-10	DFP	RGB	0.05	2021-11-10	DFP	
DTM	0.5	2023-05-02	DFP	RGB	0.05	2022-06-16	DFP	
DTM	0.2	2022-04-13	DFP	RGB	0.1	2022-04-13	DFP	
DTM	0.2	2022-09-12	DFP	RGB	0.1	2022-09-12	DFP	4
DTM	0.2	2023-05-24	DFP	RGB	0.05	2023-05-24	DFP	
DEM	0.2	2023-09-27	DFP	RGB	0.2	2023-09-27	DFP	5
DEM	0.2	2023-09-27	DFP	RGB	0.2	2024-03-02	DFP	6
Soulac implantation in 2024								
Sources: https://www.pigma.org/ (BRGM)								
DEM	1	2012-10	DFP					
DEM	1	2014-10	DFP					
DEM	1	2016-10	DFP					
DEM	1	2017-10	DFP					
DEM	1	2018-10	DFP					
DEM	1	2029-10	DFP					
DEM	1	2020-10	DFP					
DEM	1	2021-10	DFP					
DEM	1	2022-10	DFP					

DTM	*1*	*2022*	*DFP*	*RGB*	*0.1*	*2022-09*	*PAD*	
DTM	1	2023-09	DFP	RGB	0.1	2023-09	PAD	1
DTM	0.1	2024-01-16	DFP	RGB	0.05	2024-01-16	DFP	2
DTM	0.1	2024-04-23	DFP	RGB	0.05	2024-04-23	DFP	3
DTM	0.1	2024-10-24	DFP	RGB	0.05	2024-10-24	DFP	4
The Netherland								
Delftlandse kust/Zand Motor implantation in 2011, Hondsbossche Duinen implantation in 2015, Katwijk implantation in 2013/2015, Texel implantation in 2019								
Sources: https://www.beeldmateriaal.nl/ (Beeldmateriaal Nederland); https://www.ahn.nl/ (Actueel Hoogtebestand Nederland); https://rijkswaterstaatdata.nl/ (Rijkswaterstaat)								
DTM	5	1996 / 1998	PAD					
DTM	5	2005	PAD					
DTM	5	2006	PAD					
DTM	5	2007	PAD					
DTM	0.5	2007 / 2008 / 2011	PAD					
DTM	5	2008	PAD					
DTM	5	2009	PAD					
DTM	5	2010	PAD					
DTM	2	2011	PAD					
DTM	2	2012	PAD					
DTM	2	2013	PAD					
DTM	0.5	2014 / 2016 / 2017	PAD	RGB+NIR	0.25	Summer 2016	PAD	1
DTM	2	2014	PAD					
DTM	2	2013	PAD					
DTM	2	2014	PAD					
DTM	1	2015	PAD					
DTM	2	2016	PAD					
DTM	2	2017	PAD	RGB+NIR	0.25	Summer 2017	PAD	2
DTM	2	2018	PAD	RGB+NIR	0.25	Summer 2018	PAD	3
DTM	2	2019	PAD	RGB+NIR	0.25	Summer 2019	PAD	4
DTM	0.5	2020	PAD	RGB+NIR	0.25	Summer 2020	PAD	5
DTM	2	2022	PAD	RGB+NIR	0.25	Summer 2022	PAD	6
DTM	0.5	2023	PAD	RGB+NIR	0.25	Summer 2023	PAD	7
DTM	2	2024	PAD					
Sweden								
Ystad implantation date 2011								
DSM	*1*	*2019*	*DFP*	*RGB*	*0.5*	*2004*	*DFP*	
DSM	*1*	*2019*	*DFP*	*RGB*	*0.25*	*2006*	*DFP*	
DSM	*1*	*2019*	*DFP*	*RGB+NIR*	*0.5*	*2007*	*DFP*	
DSM	*1*	*2019*	*DFP*	*RGB+NIR*	*0.5*	*2010-04-15*	*DFP*	

DuneFront

DSM	1	2019	DFP	RGB	0.25	2010-06-04	DFP	1
DSM	1	2019	DFP	RGB+NIR	0.25	2012-05-02	DFP	2
DSM	1	2019	DFP	RGB+NIR	0.25	2014-03-31	DFP	3
DSM	1	2019	DFP	RGB+NIR	0.25	2016-05-13	DFP	4
DSM	1	2019	DFP	RGB+NIR	0.25	2018-04-11	DFP	5
DTM	0.1	2020-10-23	DFP					
DTM	0.1	2021-11-22	DFP					
DTM	0.1	2022-01-12	DFP					
DSM	1	2022	DFP	RGB+NIR	0.16	2022-04-18	DFP	6
DSM	2	2023	DFP					
DTM	0.1	2023-07-09	DFP					